UNIVERSITY
OF GÄVLE

FACULTY OF ENGINEERING AND SUSTAINABLE DEVELOPMENT

Department of Building, Energy and Environmental Engineering

Analysis of the energy savings gained by protective glazing on stained single-glass windows at Uppsala cathedral

Izaskun Villaro

June 2016

Master Programme in Energy Systems
Master's Thesis, 15 credits
Main field of study: Heat transfer

Supervisor: Magnus Mattsson
Examiner: Shahnaz Amiri

ABSTRACT

Most European stained glass windows have no protection to reduce the damage due to environmental exposure, and this is the case of the great gothic windows in the Uppsala Cathedral. Currently, the implementation of protective glazing systems is being carried out in order to reduce the damage of the stained glass.

In this connection, an analysis of the energy saving potential of the protective system is of great interest. The main obstacle in the implementation of this kind of systems is a social rejection based on the fact that the additional panes perturb the appearance of the historic building. Thus, demonstrating that there would actually be an energy saving, with the corresponding economic saving, would help approving the implementation of the protective glazing system.

Measurement data needed for the analysis were available since they were used in condensation studies for the damaging analysis. However, the fact that this data was not gathered thinking of the energy saving analysis and its difficulties, some limitations have appeared in the present study. Accordingly, the needed simplifications imply some uncertainty in the results. However, the reliability of the results and the conclusions that can be drawn from the analysis are contrasted with previous similar studies.

Different methods of calculation and analysis will be discussed, and finally results for the heat transfer coefficients through the open air gap and through the whole double paned system will be obtained. Furthermore, an energy saving analysis will be carried out with the winter data for both the case of the case of the *Sonens fönster* and the case of also implementing a similar system in the rosette of the cathedral. As a result, the conclusions drawn will be that the implemented protective glazing system reduces the heat losses through the windows to less than a third and that savings of about 8700 kWh/year and 13000 kWh/year are achieved in the case of the system being implemented only in *Sonenes fönster* and also in the rosette respectively.

Finally, a rough study of the condensation problem will be exposed and possible matters, along with some advices, of further studies regarding more accurate analysis of both the condensation and the energy saving analysis will be presented.

Keywords: stained glass, protective glazing, energy savings.

AKNOWLEDGEMENTS

In first place, I would like to express my sincere gratitude to my teacher and supervisor Magnus Mattsson for his continuous support and advice. His guidance has been very important in the development of the analysis as well as in the writing of the thesis.

Besides my supervisor, I would like to thank the professionals at *Svenska Kyrkan* Linda Kvarnstrom and Viktor Wadelius for their helpful collaboration and support, without which this Master's Thesis would not have been possible. Thank you for the *in-situ* explanations and the kindest attention.

Last but not least, I want to thank my colleagues at *Högskolan I Gävle* for their understanding and support along all the process and specially for the great experiences that we have shared.

TABLE OF CONTENTS

INDEX OF FIGURES

INDEX OF GRAPHS

INDEX OF TABLES

1. INTRODUCTION

1.1 Background

An extensive window renovation work is currently being performed at the great gothic cathedral in Uppsala. The ancient historic building, which stands since 1435, has large stained glass windows that show signs of severe damage after being exposed to the atmospheric conditions for a long time; mainly because of particles deposition and condensation. In this context, tests are being done on the *Sonens fönster* window by adding an outside pane with an air gap for natural air convection in between, in order to attain a warmer inner pane thus minimizing the particles deposition and the condensation on the stained glass window and reducing the need of maintenance and renovation.

The question is if the installation of these panes would really cope with the actual damaging problem but also if they would provide an additional important benefit: the reduction of the heat losses through the windows. Although this has not yet been assessed, the interest in the possible energy savings is great.

Even though a lot of research has been made regarding the conservation problem, very little investigation has focused on the thermal effectiveness of the protective glazing. The paper [1], however, offers the description and results of an experimental test called *hot box experiment* which consists in introducing the system in assemblies surrounded by insulating material with a known thermal conductivity and run tests to evaluate only the thermal performance of the window.

Given the fact that the object of study is an ancient historic building the aesthetic impact of installing the panes on the outside gives place to a lot of controversy. Therefore, revealing that apart from the preserving advantages the protective glaze system would provide energy and the corresponding money savings would help in approving its implementation.

1.2 Problem description

The problem consists in analysing the installed protective glazing system, which provides the window with a second pane, in terms of thermal behavior and estimate the reduction in heat losses in order to assess the energy savings. The configuration to be analysed can be seen in Figure 1c.

Even though specific experimental tests of heat transfer would be a more reliable and easy way to study the thermal behavior of the system, in this thesis the only possibility is to analyse experimental data gathered by the professionals of *Svenska Kyrkan* during an assessment on the condensation problem that is strongly related to the conservation of the stained glass. Therefore, in order to fulfill the objectives of the thesis, publications about analytical relations for natural convection heat transfer coefficients for the considered configuration, such as [2], [3] and [4], need to be studied and the most appropriate analytical methodology has to be chosen. In

addition, procedures based on the available experimental data need to be included in the analysis in order to provide objective and realistic results.

1.3 Objectives

The thesis work intends to make this energetic assessment through theoretical analysis of the heat transfer through the double glazed system with the available data gathered by the professionals at *Svenska Kyrkan*. In the development of the theoretical analysis the overall heat transfer coefficient through the windows must be calculated as it is the most meaningful parameter in the heat loss and energy saving calculations. In addition, the likeliness of condensation taking place must be discussed.

Moreover, the results obtained in the different methods of analysis have to be discussed and the best way to proceed in the energetic assessment with the available data has to be determined. Besides, since the future implementation of a similar protective glazing system on the stained rosette of the cathedral is being considered, it is interesting to include the effect it would have in the energetic assessment.

Finally, the condensation problem will be studied and discussed and some observations and suggestions will be given for further studies.

1.4 Delimitations

The main limitations in achieving valid results are the accuracy of the available measuring instrumentation. Also, environmental factors such as sun radiation can jeopardise the results because of the heat up the sensors which results in false measurements. In fact, the window at Uppsala Cathedral involved in the analysis is the *Sonens fönster* (see Figure 2) and It is oriented to the south. Consequently, solar radiation has a greater effect than in other windows placed in differently oriented facades. Its location in the building of the cathedral can be appreciated in Appendix I.

This is why the data had to be revised in order to select the valid measurements and as a result fewer data than expected was used in the analysis. In addition, the fact that the measurements were not made for the energy analysis but for the condensation one is another limitation for the information available for the present study. Last but not least, the approximations and hypothesis undertaken in the different methods of analysis are sources of more uncertainties.

1.5 Disposition

The thesis starts with a literature review containing relevant information for the analysis. Then, considering the data available to address the problem different calculation methods are identified and the results obtained are compared and discussed. Right after, the energy savings achieved in the year corresponding to the data gathering (2015) are estimated and the condensation problem is studied in two different ways. Finally, some conclusions regarding the energy saving and the condensation analysis are drawn and some observations and suggestions for further studies are given.

2. THEORETICAL FRAMEWORK

2.1 System configuration and construction details

Basically, as shown in Figure 1 there are four varieties of protective glazing systems regarding the air flow between the two panes; non-ventilated, externally ventilated, internally ventilated and mixed-ventilation [5].

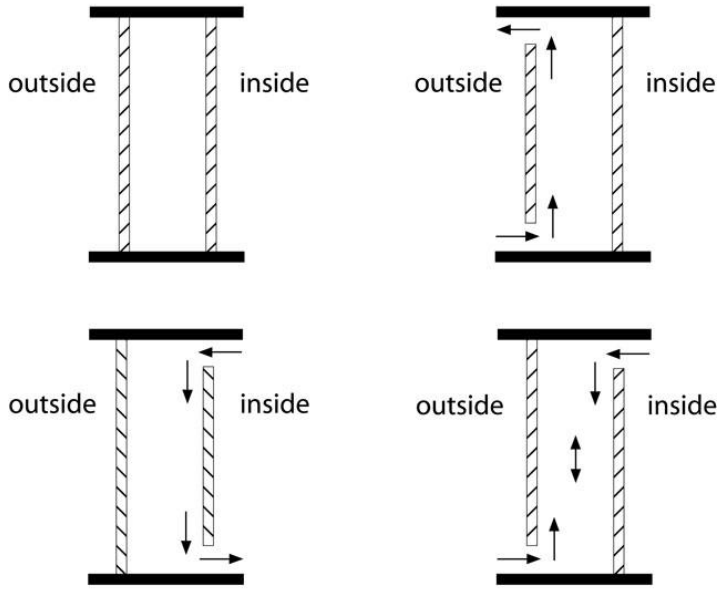

Figure 1: Types of ventilation system: (a) non-ventilated, (b) externally ventilated, (c) internally ventilated, and (d) mixed-ventilation systems [5].

As previous research shows that it is the system that best protects the historical glass from degradation [6], the system installed in Uppsala Cathedral is of the internally ventilated kind, also known as isothermal protective glass system. In this configuration, the indoor air of the cathedral flows in the channel between the two panes due to the existing buoyancy and mainly warming up the inner surface of the outer pane by means of natural convection. As a result of the stained glass being in contact with indoor air on both sides, the temperature on its two surfaces is higher than when it stands alone and in contact with the outdoor air on one side and with indoor air on the other side. Along with these higher temperatures comes an important decrease in the condensation of the water vapor present in the air and therefore a lower corrosion of the stained glass that leads to a minor need of maintenance and renovation.

The *Sonens* window Figure 2a consists of different glass pieces coupled to a stone structure. These different pieces are sketched in Figure 2b, where it can be seen that most of the area of the window is composed of two rows of long glass units separated from each other by the stone framing. Moreover, these considered units are isolated and far enough from each other so as to have independent air flows in their respective channels. Therefore, the convective phenomenon that occurs in each of them must be studied separately. A view from the outside can also be observed in Figure 2c.

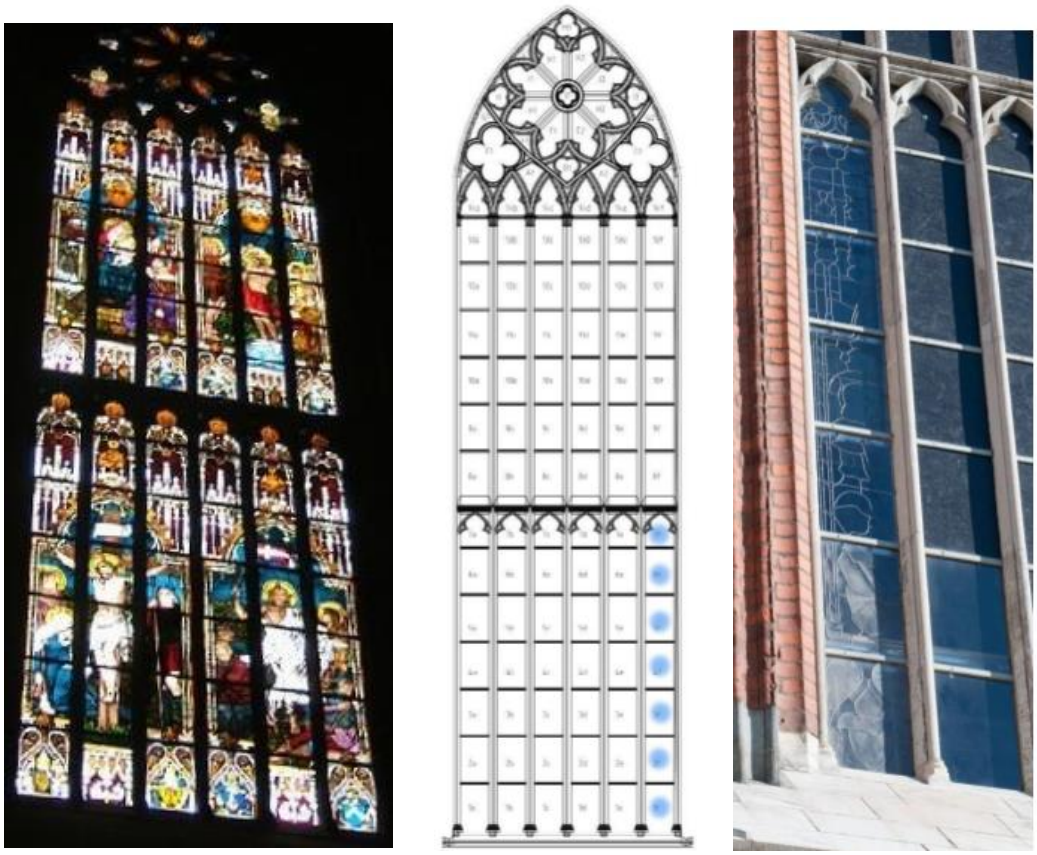

Figure 2: *Sonens fönster* (a) view of the stained glass from the inside, (b) scheme of the stained glass, (c) view of the window from the outside.

The upper slot, shown in Figure 3, has a complex geometry. It can also be seen how, as it was mentioned before, these glass units are integrated in a stone structure and the air inlets and outlets are far enough to study them independently.

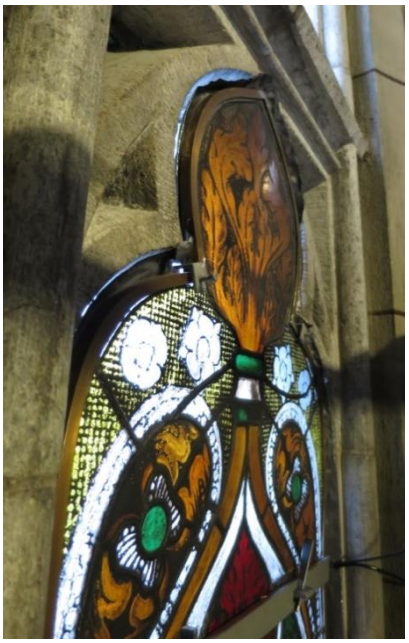

Figure 3: detail of the top slot in one of the stained glass window panes.

The details of the lower part of the space between panes can be observed in Figure 4. Different distances between panes have been applied in order to find the configuration that presents the best performance, and that is why the space between panes shown in Figure 4 differs from the current one which is the one used in the analysis. Currently, the stained glass is placed at a 60 mm distance from the protective glazing.

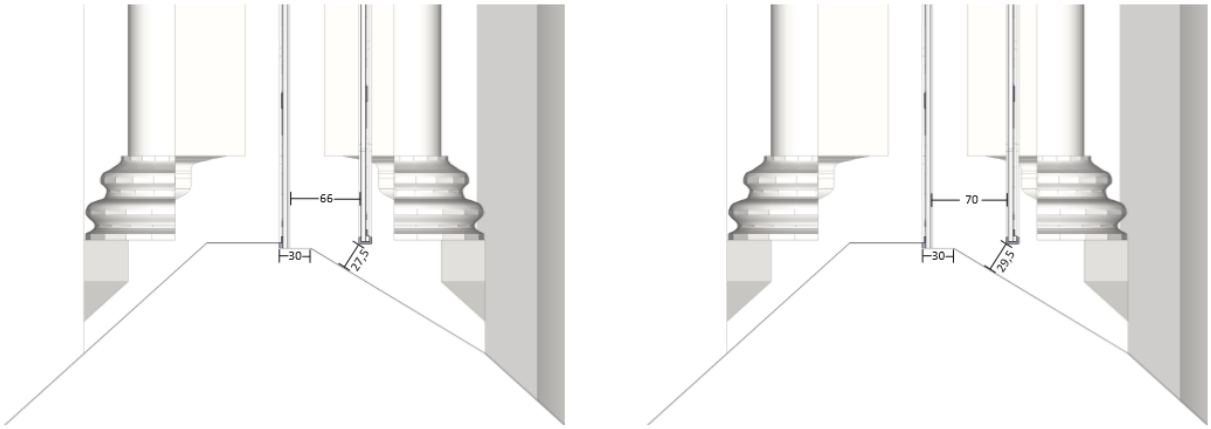

Figure 4: constructive detail of the lower part of the space between panes.

2.2 Heat transfer principles

2.2.1 Natural convection

The phenomenon that takes place between the two vertical panes is natural convection. The air from the inside of the cathedral moves through the gap between the panes due to the temperature difference between the indoor space of the cathedral and the surfaces of the panes facing the gap. When the temperature of these surfaces is higher than the one inside the cathedral, the ambient air enters the channel from the lower slot and rises due to the buoyancy, being heated by the hot plates in the process. However, when the temperature of the surfaces is lower than the ambient air in the cathedral, the air enters the channel through the upper slot and flows downwards to the lower slot instead, being cooled in the process.

In the gap, the boundary layers start to develop at the inlet of the fluid (upper or lower slot depending on the buoyancy) and eventually merge if the plates are long enough and not too far from each other. If this is the case, the flow after the merger will be fully developed and it is correct to analyse the natural convection flow as channel flow. Nevertheless, if the plates are not long enough or the space between them is too large the boundary layers corresponding to the two opposing surfaces never merge. Therefore, the natural convection flow on the surface of one of the plates is not affected by the presence of the other plate. In this case, the problem should be solved by analysing the convection on each of the plates independently [7].

In addition, it is known that in the case of two isothermal parallel plates with the same temperature on the surfaces facing the gap the boundary layers merge at the midplane

of the interspace (see Figure 5). This is the case of the natural ventilation of finned surfaces and PCBs, where some heat needs to be extracted from the fins, which are at a determined temperature, by means of the air natural movement caused by the existing buoyancy.

If the two surfaces facing the gap do not have the same temperature, as it happens in the case studied in this paper; the boundary layers merge at a different plane. However, there still is a full developed flow after the merge so the flow must also be studied as a channel flow [7].

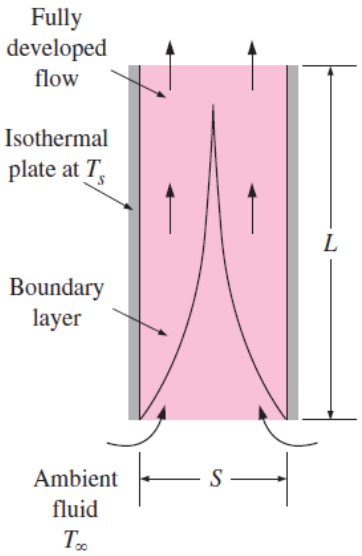

Figure 5: natural convection flow through a channel between two isothermal vertical plates [7].

In order to analyse the natural convection some relations, based on the dimensionless parameters Nusselt, Rayleigh, Grashof and Prandlt, are used.

The Grashof number represents the ratio of the buoyancy force to the viscous force, and it is the one that governs the flow regime in natural convection. It is used to determine whether the regime of the fluid is laminar or turbulent, and it can be obtained as:

$$Gr_L = \frac{g\beta(T_s - T_\infty){L_c}^3}{\nu^2} \qquad (1)$$

Where
g= gravitational acceleration [m/s^2]
β= coefficient of volume expansion [1/K] ($\beta = 1/T$ for ideal gases)
T_s= temperature of the surface [ºC]
T_∞= temperature of the fluid sufficiently far from the surface [ºC]
L_c = characteristic length of the geometry [m]
ν= kinematic viscosity of the fluid [m^2/s]

Note that the subindex "L" in the Grashof number indicates that it is related to the characteristic length of the geometry "L_c". Another way to define the Grashof number

is in terms of the characteristic surface instead, and then the subindex would be "s" instead.

In this calculation all the fluid properties must be evaluated at the film temperature, which is defined as the mean temperature between the surface temperature and the temperature of the fluid sufficiently far from the surface:

$$T_f = \frac{(T_s + T_\infty)}{2} \qquad (2)$$

On the one hand, the average Nusselt number in natural convection has been defined out of empirical correlations as:

$$Nu = \frac{h \cdot L_c}{k} \qquad (3)$$

Where
h = convection coefficient of heat transfer [W/m^{2}K]
k = thermal conductivity [W/mK]

And it is usually expressed in terms of the Rayleigh number (kinematic viscosity of the fluid divided by its thermal diffusivity), a constant coefficient and a constant exponent. In addition, the relation that defines the Rayleigh number $Ra_L = Gr_L \cdot Pr$ can be used [7].

$$Nu = \frac{h \cdot L_c}{k} = C \cdot (Gr_L \cdot Pr)^n = C \cdot {Ra_L}^n \qquad (4)$$

Where
C= constant coefficient
n= constant exponent

And again, the subindex "L" in the Rayleigh number indicates that it is obtained out of the $\mathrm{Gr_L}$ related to the characteristic length of geometry $\mathrm{L_c}$. The constant coefficient C and the constant exponent n are determined experimentally. However, it is known that the n is usually $\frac{1}{4}$ for laminar flow and $\frac{1}{3}$ for turbulent flow and that the C is normally less than 1.

Natural convection heat transfer depends on the geometry of the surfaces involved and their orientation, but also on the temperature variation on the surfaces and the thermophysical properties of the fluid. Therefore, even though the mechanism of natural convection is well understood, the complexity of fluid motion makes it difficult to solve the governing equations of motion and energy in order to obtain analytical relations for the Nusselt number, which is the one related to the heat transfer coefficient h.

Therefore, except from some simple cases, such as the one of finned surfaces and PCBs, heat transfer relations for natural convection are obtained from experimental studies. Regarding the case studied in this paper, [2] establishes relations for the

Nusselt number for both panes from a deep differential study of the air motion and heat transfer. Their validity is justified by comparison with the previous studies made by Chan and Tien [8] and Zimmerman and Acharya [9], and the influence of the Rayleigh number, the size of the openings and the thermal conductivity of the bounding wall were examined.

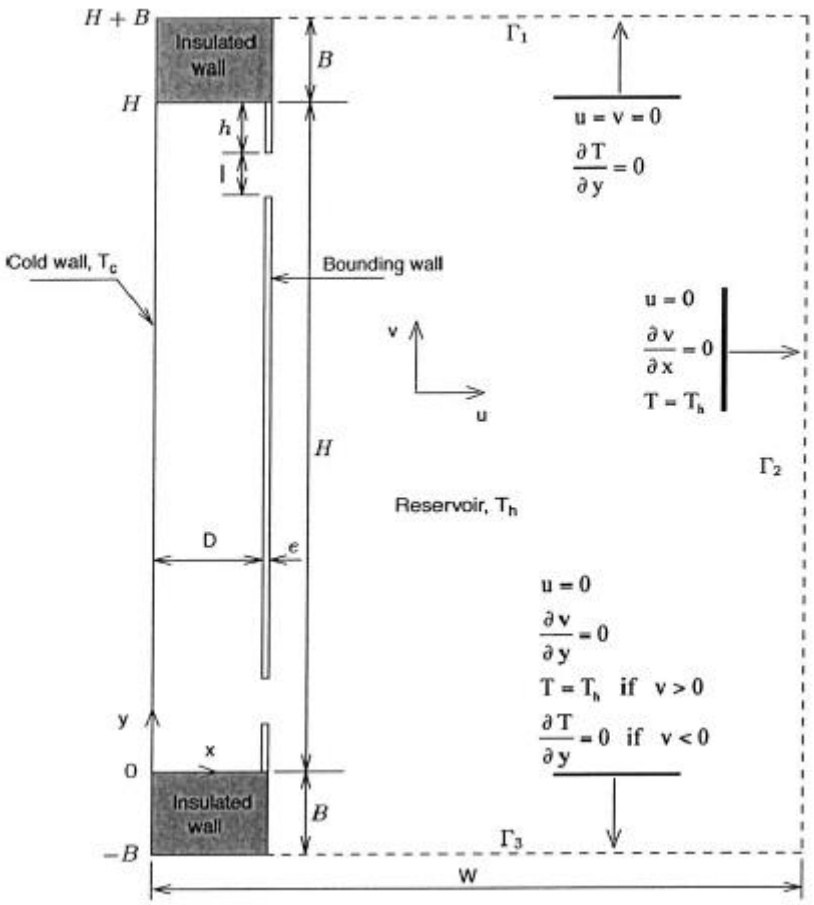

Figure 6: scheme of the parameters involved in the natural convection problem [2].

The interesting relation for the Nusselt number is the one for the outer pane (cold wall in the picture above). In this article [2] two relations are given, depending on the value of the thermal conductivity ratio between the wall (or pane) and the fluid:

$$Nu_c = \left(\left(\frac{13.33}{Ra_D} \right)^2 + \left(\frac{1}{0.546 \cdot Ra_D} \right)^2 \right)^{-\frac{1}{2}} \quad for\ N_k \to 0 \qquad (5)$$

$$Nu_c = \left(\left(\frac{2.78}{Ra_D^{\frac{1}{2}}} \right)^{\frac{5}{2}} + \left(\frac{1}{0.546 \cdot Ra_D^{\frac{1}{4}}} \right)^{\frac{5}{2}} \right)^{-\frac{1}{2}} \quad for\ N_k \to \infty \qquad (6)$$

$$N_k = \frac{k_w}{k_f} \qquad (7)$$

Where:
Ra_D= Rayleigh number in terms of the width of the channel [-]
N_k= thermal conductivity ratio [-]
k_w= thermal conductivity of the wall [W/mK]
k_f= thermal conductivity of the fluid [W/mK]

Once the Nusselt number is calculated the convective heat transfer coefficient can be determined from equation (3) and therefore the heat released by the indoor air to the cold pane from the following expression:

$$\dot{Q}_{loss} = h \cdot A \cdot (T_\infty - T_c) \qquad (8)$$

Where
A= Area of the pane [m^2]
T_∞= Indoor air temperature [ºC]
T_c = Temperature of the cold (outer) pane [ºC]

2.2.2 Heat transfer in windows

There are many different kinds of windows, and because the heat transfer is influenced by the indoor and outdoor conditions, the glazing construction (such as the number of glazing panes), the gas-space dimensions, the orientation relative to vertical, the emittance and conductance of the materials and the composition of the gas [10], each case must be studied in order to draw conclusions about the thermal performance.

In order to evaluate the rate of heat transfer through a window, and also to compare the thermal performance of different windows, the overall U-factor is commonly used in the building sector as it can be observed in several guidebooks and literature e.g. [7] and [8]. It relates the total heat transfer with the temperature difference between the inside of the building and the surrounding environment.

$$\dot{Q}_{loss} = U_0 \cdot A \cdot (T_i - T_e) \qquad (9)$$

Where
U_0= overall U-factor [W/m^{2}K]
T_i= indoor air temperature [K]
T_e= outdoor air temperature [K]

In this paper, despite the fact that an easier and more accurate way to obtain the overall U-factor of historical glasses with protective systems is to test the performance of the system experimentally, as it was done in the case of the stained glass at Swiss parish churches [1], it will be estimated analytically. In order to do so, the different heat transfer phenomena that occur must be understood and evaluated.

Even though big efforts have been made in analising the natural convection that occurs in the channel in the configuration presented in Figure 5, and a couple of valid relations for the Nusselt number have been obtained and can be found in several

articles, in order to study the heat transfer through the window the radiation between the glass surfaces and their surroundings must also be taken into account.

Usually, the effects of convection and radiation on the inner and outer surfaces of glazings are combined in one heat transfer coefficient; h_i for the inner surface and h_o for the outer one.

According to [7], if the air inside the room can be considered as still the combined heat transfer coefficient for the inner surface of a vertical window can be obtained from the expression below, where the temperatures raised to the fourth power must be introduced in Kelvin:

$$h_i = h_{conv} + h_{rad} = 1.77 \cdot (T_g - T_i)^{0.25} + \frac{\varepsilon_g \cdot \sigma \cdot ({T_g}^4 - {T_i}^4)}{T_g - T_i} \qquad (10)$$

Where
h_i= combined heat transfer coefficient for the inner surface [W/m^{2}K]
ε_g= emissivity of the inner surface [-]
σ= 5.67·10^{-8} [W/m^{2}K^4], Stefan-Boltzman constant
T_g= glass temperature [K]
T_i= indoor air temperature [K]

In (10) all the surfaces facing the window are assumed to have the same temperature as the indoor air. This simplification is reasonable when they are mostly interior walls, but it becomes questionable when the window is exposed to heated or cooled surfaces or to other windows.

On the other hand, the value of the combined heat transfer coefficient for the outer surface of the window depends strongly on the wind. Several relations exist for the convective part, where the influence of the air speed lies. However it has no sense to suppose a random wind speed given the fact that there already are estimations for the exterior combined heat transfer coefficient; some based on an annual mean value of the wind speed and some regarding only winter conditions [10]. In this study, as in order to analise the energy savings the winter case is the most important one, the last ones are more adequate.

Moreover, in the case of double glazing radiation takes place between the two surfaces facing the air gap. When the effects of the edges of the glazing are negligible, the radiation heat transfer between two large plates at absolute temperatures and follows the expression:

$$\dot{Q}_{rad} = \frac{\sigma \cdot A \cdot ({T_1}^4 - {T_2}^4)}{1/\varepsilon_1 + 1/\varepsilon_2 - 1} = \varepsilon_{effective} \cdot \sigma \cdot A \cdot \left({T_1}^4 - {T_2}^4\right) \qquad (11)$$

Where ε_1 and ε_2 are the emissivity factors of the two facing surfaces and the effective emissivity is expressed as

$$\varepsilon_{effective} = \frac{1}{1/\varepsilon_1 + 1/\varepsilon_2 - 1} \qquad (12)$$

In addition, the frame of the window and the spacers between glasses placed to provide edge seal as well as uniform spacing serve as undesirable “thermal bridges”. This will increase the heat transfer because of the higher thermal conductance of the materials involved (metal in this case) and hence the influence of these elements must be evaluated. There already are tabulated values for different overall U-factors for some kind of windows, with or without frame and depending on the material of the frame [7]. From existing data like that and literature on the analysis of the two-dimensional heat transfer that take place in the edges and frames of windows some rough conclusions can be made.

2.3 Preservation of historical stained-glass windows

The main problem affecting the preservation of historical stained-glass windows is condensation. When water present in the ambient air condensates on the surfaces of the glass, chemical reactions that provoke its weathering occur. The main reaction is based on ion exchange and it causes the formation of a gel layer, low in alkaline ions but rich in protons and water. If this layer reaches a certain thickness, thermal and hygric stresses will cause micro-cracks, allowing more access for harmful substances to penetrate deeper into the materials. Besides, air pollutants, dust and micro-organisms accelerate the process [11].

According to [11], the most affected cases are medieval glasses presenting a relatively high content in potassium and calcium and in more stable glass from the 19th century the major degradation lies in the loss of paint. In Figure 7 an example of degradation of a stained-glass window at Uppsala Cathedral is exhibited.

Figure 7: example of degradation in a stained glass window at Uppsala Cathedral.

Apart from the water vapour content in the air, there are other factors that cause the weathering of the glass, such as contaminants present in the air. In fact, atmospheric pollutants; gases as well as particles, have been identified as the major cause of the weathering of historic stained glass windows [12]. Fortunately, even though experts in

conservation have not succeed in stopping or reversing the ensuing damage so far, a slower rate of destruction is certainly achievable by installing a protective glazing system [13].

The main concern about particles deposition is the fact that it significantly changes the dew point, i.e. the temperature at which water vapour condenses on the glass [13]. Besides, water-soluble salts and carbon-containing particles are also of great concern because while the former have the capability to maintain a high humidity on the glass surface during relatively dry periods, the latter constitutes a potential source of food for many microorganisms [14].

In addition, gaseous air pollutants can be dangerous for the stained glass. The most harmful ones are sulphur dioxide (SO_2), nitrogen dioxide (NO_2), and ozone (O_3) and they are mostly derived from anthropogenic sources [14]. One of the advantages of the internally ventilated protective glazing systems is that, given the fact that the outdoor concentrations of SO_2 are usually higher than the ones inside the building [15], now that the protective glass is placed in the original location of the stained glass and this one is placed in an inner position the exposition of the stained glass to this contaminant is highly reduced.

Despite the presence of air pollutants and because of the important influence of the condensation in the weathering of the historical glass, the values of relative humidity inside the building and in the interspace between panes is a key factor determining the preservation of the historic stained-glass [14].

The most effective way to avoid condensation on the glass is to provide sufficient ventilation, and it can be optimized with a good design of the system regarding the cross-sectional area of the air channel; the distance between the original and the protective glazing (5 to 10 cm in general) as well as the openings at the top and at the bottom [14]. The air flow in the gap determines the relative humidity and also the transport of particles and their deposition on the glass. According to [16], the values of the average air velocity of an effective protective glass system should be between 0.1 and 0.34 m/s most of the time.

Finally, it has to be said that the stained glass handling high temperatures is also damaging. According to [16] the glass temperature should not exceed 30 °C provided that above this limit the degradation increases remarkably. Since the *Sonens fönster* is facing south, the temperature of its surfaces trespasses this limit more often than windows orientated in other direction and the protective glazing is expected to reduce the time that the historical glass is subjected to such high temperatures. Nevertheless, given the lack of data during the summer period the time that the historical glass handles these temperatures can not be assessed, and hence this analysis necessarily remains for further studies.

3. METHOD

3.1 Data treatment

The data available consists of different measurements recorded every thirty minutes along the year 2015. The sensors measured the temperatures on the inner and outer surface of the historical glass, on the inner one of the protective pane, in the inside of the cathedral, in the outside and also right in the middle of the air gap between the panes, as well as the air velocity in that same point. Besides, the temperature measurements were taken at two different heights on the glass surfaces and in the air gap, and the air velocity measurements at three different heights (see Appendix II).

Even though there is data available for the whole year, since the aim of the study is to provide information about the energy savings the interesting period is the one when there is heating consumption. Consequently, the analysis focuses on the winter season. Furthermore, some clear errors in some measurements were detected e.g. glass temperatures suddenly rising from around 15°C to 30°C or even 40°C and the corresponding data was not considered in the analysis.

Moreover, physical properties of the two different kinds of glass such as conductivity and emissivity have been given, along with their thickness and other construction details. In addition, the rest of the needed dimensions of the window can be obtained from the given blueprint as exposed in Appendix III.

Finally, once all the needed data was gathered the problem could be addressed. On the one hand, the EES software was used in order to provide the thermophysical properties of air and water vapour and also to solve most of the equations, especially the ones regarding heat transfer. On the other hand, some other calculations and data treatment needed were made in Excel.

3.2 Analysis of the improvement in thermal behavior compared to the case of a single pane

The problem consisting of calculating the heat loss through the window in the installed system can be solved in different ways, and the benefits and reliability of each method have to be discussed.

Firstly, the heat loss through the window can be characterized by thermal resistances as it is illustrated in Figure 8, Figure 9 and Figure 10. Therefore, one way to analyse the improvement in thermal behavior, exposed in section 3.2.1, will be to compare the total resistance to heat transfer between the inside (T_∞) and the outside (T_{out}) of the cathedral with and without the protective system installed. Due to the complexity of the heat transfer occurring in the system installed, there are different heat balances that can be analysed depending on the definition of the control volume. Therefore, there will be different ways to assess the total heat flow through the window and as a result different estimations of the overall U-factor.

However, the case of the stained glass standing alone is simple, and there is only one heat balance that can provide the overall U-factor. Therefore, the different methodologies will consist in calculating the overall U-factor for the installed system in different ways and then contrast them with the one obtained for the historical glass alone.

3.2.1 Heat resistance of the stained glass alone

When the historical glass stands alone the heat transfer case to address is the following: there is convective heat being transferred from the warmer indoor air and also radiation from the different surfaces inside the cathedral facing the stained glass that reach its inner surface. The total heat that reaches this inner surface is transferred by means of conduction through the glass to the outer surface, and finally to the environment both due to convection and radiation.

Three different resistances can be defined; one for the total heat that reaches the inner surface of the glass, one for the conduction that takes place along the thickness of the pane and a third one characterizing the heat transfer from the outer surface to the surrounding environment. The first resistance is the inverse of the combined heat transfer coefficient that can be obtained from (10), the resistance to conduction is the inverse of the conductivity of the historical glass and the last resistance is the inverse of the combined heat transfer coefficient for the exterior surface that can be assessed from existing literature.

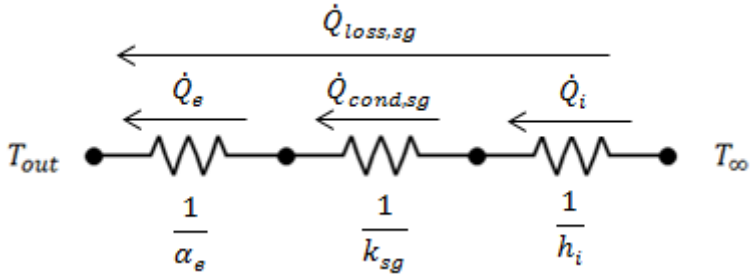

Figure 8: scheme of the thermal resistances in the case of the stained glass alone

As the result is a configuration in series, the resistances can be added in order to obtain a global resistance between the temperatures inside (T_∞) and the outside (T_{out}) of the cathedral. Certainly, the inverse of the mentioned global resistance is the overall U-factor when the historical glass stands alone U_{sg}.

$$\frac{1}{U_{sg}} = \left(\frac{1}{\alpha_e} + \frac{1}{k_{sg}} + \frac{1}{h_i}\right) \qquad (13)$$

Given the lack of data from any analysis on the stained glass standing alone, the surface temperature of the glass used in order to assess the h_i has been an estimation. This estimation has been based on the given data for the protective system and on the fact that the thickness and conductivity of both the protective ad the stained glass are almost the same. The approximation consists in considering the temperature of the

inner surface of the stained glass to be the one outside plus 1.7°C. The validity of this assumption lies in the fact that small variations in this temperature would not affect the result obtained for the h_i considerably, and the need of obtaining the overall U-factor in this case justifies the simplification

3.2.2 Method 1: Comparison of the global heat resistances before and after the implementation of the protective glazing

The first way to calculate an overall U-factor for the installed system will also be defining the different thermal resistances related to the different heat transfers in order to obtain a global one between the indoor and outdoor temperatures.

With the implementation of the protective glazing system, the case becomes more complicated mainly due to the natural convection occurring between the two panes. If the convective heat transfer coefficient obtained in the equations (5) and (3) is used, the radiation heat exchange with the interior surfaces of the cathedral facing the stained glass is neglected. This is so because the convective heat transfer coefficient refers to the total convective heat that is released to the cold pane, obtained analytically from fluid mechanics and heat transfer equations without considering any of the radiative interactions.

In the real case there is radiation from the interior surfaces of the cathedral (which can be considered to be at the temperature T_∞) to the inner surface of the inner pane (stained historical glass at a temperature $T_{sg,i}$), and also from the outer surface of the stained glass (at temperature $T_{sg,o}$) to the inner one of the protective glass (at temperature ($T_{c,i}$)). On the one hand, the effect of radiation from the interior surfaces of the cathedral is raising the temperature of the stained glass and this necessarily increases the convective heat transferred to the protective glazing. Besides, it also increases the radiation from the stained to the protective glass. As it will be demonstrated, the effect of radiation is small and it is partially or totally included in the next two methodologies which are based on heat balances in a control volume.

The problem is schematised in Figure 9 below. The radiative and convective heat that reaches the stained glass is transferred by means of conduction to the outer surface of the stained glass (at temperature $T_{sg,o}$), and from there by means of radiation and convection to the inner surface of the protective glass (at temperature $T_{c,i}$). The difficulty in including radiation lies in the fact that it is later partly transferred by means of convection inside the space between panes. Due to the fact that the convection is strongly provoked by the thermal buoyancy related to the indoor temperature, there is not a way to determine the convective resistance between the two surfaces facing the gap. That is why the convection needs to be evaluated using the coefficient obtained in (5) and (3), and it is not possible to add the increase in convection heat transfer related to the increment in temperature $T_{sg,o}$. Therefore, even though it looks like R_2 and R_3 can be summed, given that they are in series, and then added to R_1 in parallel it is not possible because there is no analytical way to calculate R_3.

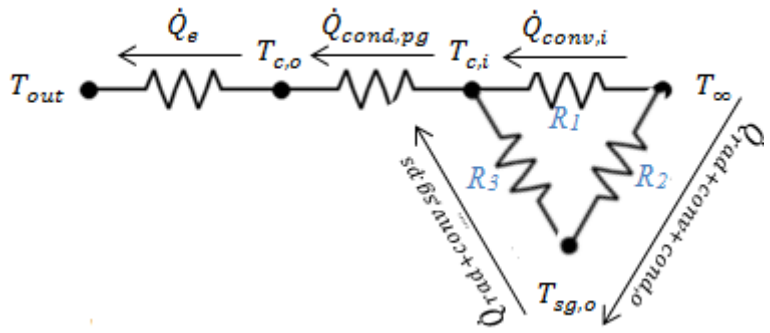

Figure 9: scheme of all the thermal resistances in the case of the double pane

Accordingly, as in [2] radiation inside the cathedral is neglected, and the resulting system of thermal resistances (Figure 10) is similar as in the case of the stained glass alone:

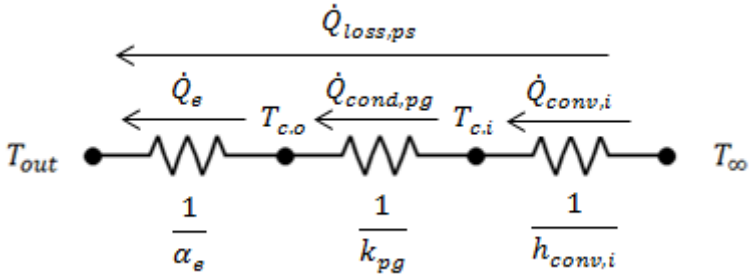

Figure 10: scheme of the resistances neglecting radiation in the case of double pane

The overall U-factor in this case is calculated as:

$$\frac{1}{U_{ps}} = \left(\frac{1}{\alpha_e} + \frac{1}{k_{pg}} + \frac{1}{h_{conv,i}}\right) \qquad (14)$$

Where the $h_{conv,i}$ (which can be obtained from equations (5) and (3)) is the global heat transfer coefficient, specially designed for the configuration of the system, between the indoor air and the surface of the protective glazing facing the channel.

As it will be discussed, the effect of the radiation emitted from the warmer surface facing the gap to the cooler one is small in comparison with the heat it receives by means of convection. Consequently, the comparison of the values obtained for the U_{sg} and the U_{ps} allows to distinguish the difference in thermal performance between the two systems.

3.2.3 Method 2: Heat balance in the control volume containing the protective glazing and the historical glass

It is possible to include radiation analising the heat balance in the control volume *V* shown in Figure 11.

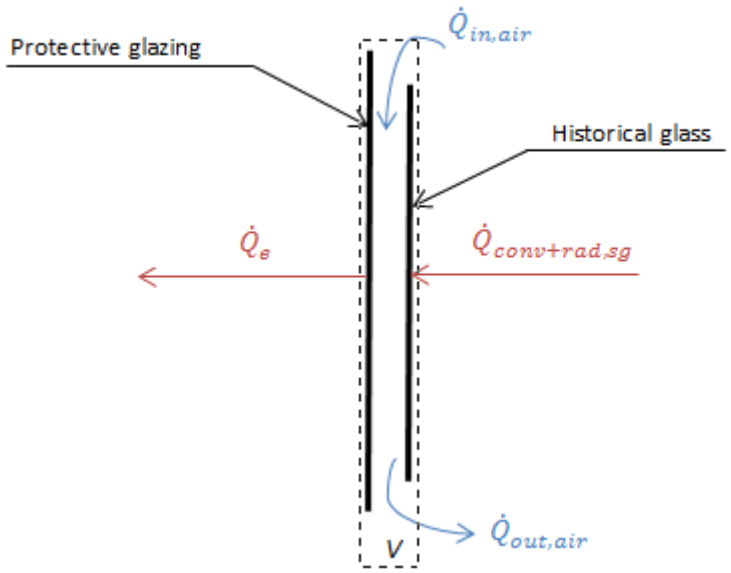

Figure 11: representation of the heat balance in the control volume containing both glasses

In order to calculate the total heat flow that reaches the inner surface of the stained glass, by means of convection and radiation, the global heat transfer coefficient can be obtained from equation (10). Also, the heat that the air releases on its way through the channel can be assessed from the temperature and speed measurements available.

Conservation of energy in the control volume *V* implies that the sum of these two heat flows equals the heat emitted from the outer surface of the protective glazing.

$$\dot{Q}_{conv+rad,sg} + \dot{Q}_{in,air} - \dot{Q}_{out,air} = \dot{Q}_e \qquad (15)$$

Moreover, the difference in energy content in the air flow between the inlet and the outlet can be calculated as:

$$\Delta\dot{Q}_{air} = \dot{Q}_{in,air} - \dot{Q}_{out,air} = \dot{m}_a \cdot c_{p,ha} \cdot \Delta T_{air} = \dot{v}_a \cdot \rho_a \cdot c_{p,ha} \cdot \Delta T_{air} \qquad (16)$$

Since the mass of air that flows through the space between panes is humid air, i.e. a mixture of dry air and water vapour, the parameters in equation (16) need to be calculated as described in [17]:

The first step is to calculate the absolute humidity ω, using the available data of temperature and relative humidity during the winter period and considering that the pressure in the channel is around 1 atm.

$$\omega = \frac{m_v}{m_a} = \frac{M_v \cdot N_v}{M_a \cdot N_a} = 0.622 \cdot \frac{P_v}{P_a} = 0.622 \cdot \frac{P_v}{1 - P_v} = 0.622 \cdot \frac{\varphi \cdot P_s}{P - \varphi \cdot P_s} \qquad (17)$$

Then, the specific heat can be obtained from:

$$c_{p,ha} = c_{p,a} + \omega \cdot c_{p,v} \qquad (18)$$

Moreover, in the analysed range of temperatures the $c_{p,a}$ and the $c_{p,v}$ can be considered to be constant. Therefore, introducing the acceptable values of 1.005 and 1.82 kJ/kg·K respectively the equation is reduced to:

$$c_{p,ha} = 1.005 + \omega \cdot 1.82 \qquad (19)$$

Where the specific heat of the mixture is expressed in terms of kilograms of dry air, and therefore the mass flow, and consequently the density, that must be introduced in equation (16) is necessarily the one of the dry air.

Finally, the volumetric air flow $\dot{v}_{air}$ needs to be estimated from the speed measurements and the known cross section of the channel. In the real case, given the fact that the temperature in the fluid is not homogeneous in every cross sectional area and it is higher in the region close to the stained glass than in the one close to the protective glass instead, a differential equation regarding this would be more accurate in the result of the volumetric air flow. However, because of the lack of data to proceed with differential equations, the equation (20) will be used instead, knowing that since it is a simplification, it is a source of error.

$$\dot{v}_{air} = u_{ave} \cdot A_c \qquad (20)$$

The air velocity is measured in the middle of the distance between the two panes, where if the regime is laminar and the flow is fully developed the speed reaches its maximum value, as shown in Figure 12. The speed needed in equation (20), however, is the average speed and according to [18] the average and maximum velocities in the case of the fluid flowing between two infinite parallel plates are related as follows:

$$u_{ave} = \frac{2}{3} \cdot u_{max} \qquad (21)$$

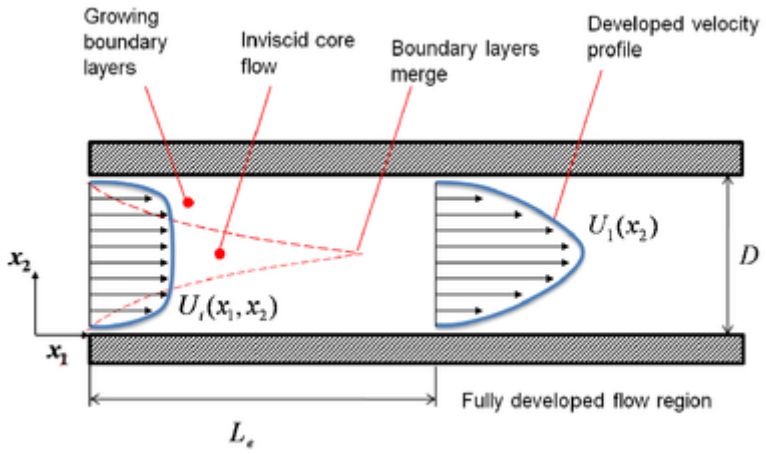

Figure 12: illustration of the air velocity distribution in the channel between two infinite plates [20]

Once the combined convective and radiative heat transfer to the inner pane and the heat released by the air are calculated the total heat flow from the inside to the outside of the cathedral can be obtained as the sum of both. Therefore, an overall U-factor that includes the effect of radiation can be assessed:

$$\dot{Q}_e = \dot{Q}_{conv+rad,sg} + \Delta\dot{Q}_{air} \qquad (22)$$

$$U_{ps} = \frac{\dot{Q}_e}{A \cdot (T_\infty - T_{out})} \qquad (23)$$

These two different methods provide U_{ps} values to contrast with the overall U-factor of the stained glass alone in order to establish if there exists an improvement in the thermal behavior of the window that leads to a reduction in the heat losses and as a consequence energy savings in the heating system at Uppsala cathedral.

3.2.4 Method 3: Heat balance in the protective glass

In addition, another heat balance (see Figure 13) can be propounded. In this case, the sum of the convective heat transfer from the indoor air of the cathedral to the protective glazing and the radiative net heat that reaches the same surface from the outer surface of the historical glass, matches the total heat flow that goes out the window $\dot{Q}_e$.

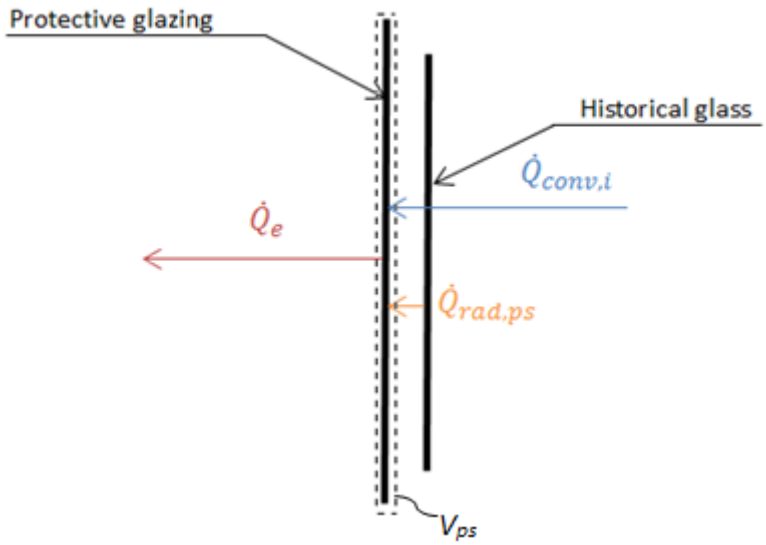

Figure 13: representation of the heat balance in the control volume containing only the protective glass

As a result, the overall U-factor for the installed system is obtained in a different way that implies parts of the two distinct methods applied before; on the one hand the convective heat is obtained from the coefficient calculated from equations (5) and (3), and on the other hand the radiative heat flow is given by the equation (11).

3.2.5 Estimation of the energy savings provided in one year

Once the new and the old overall U-factors are assessed, a first estimation of the energy savings can be made considering the total area of window provided with the protective glazing system.

The saved energy can be calculated as the difference between the heat that would be lost in the case of the stained glass standing alone and the heat losses with the protective glazing system, during the winter period since it is when the heating system is working. Hence, since the data available are taken every half an hour the saved heat in kWh/year can be achieved by multiplying the instant power obtained with each measurement by the 30min·60s/min seconds related to each measurement and dividing by 24·3600s/h as it is expressed the equation (24) below

$$Q_{saved} = \sum_{winter} \left(U_{sg,i} - U_{ps,i}\right) \cdot A \cdot (T_{\infty,i} - T_{e,i}) \cdot \frac{30 \cdot 60}{3600} \qquad (24)$$

Where
A= total area of the window [m^2]
$U_{sg,i}$= instant value of the overall U-factor of the stained glass alone [$W/m^2 \cdot K$]
$U_{ps,i}$= instant value of the overall U-factor with the protective system [$W/m^2 \cdot K$]
$T_{e,i}$= instant value of the outdoor temperature during the winter season [°C]
$T_{\infty,i}$= instant value of for the indoor temperature in the same period [°C]

Additionally, since the implementation of a similar protective system on the rosette at Uppsala Cathedral shown in Figure 14 is being considered, the effect of this measure can be added by considering the area of both windows.

Figure 14: picture of the rosette at Uppsala Cathedral

3.3 Evaluation of the risk of condensation in the new system

Even though all the pollutants exposed in the theoretical background take part in the corruption of the stained-glass, as their concentration in the environment as well as the composition of the glass differs in every case, a specific study must be carried out in order to determine their effect. The lack of this kind of data record, along with the fact that the Uppsala Cathedral is located in a cold climate where condensation induced by low temperatures of the glass surfaces is expected to be likely, will lead to not analysing the effect of the air pollutants.

Instead, the analysis will be based on the measurements of relative humidity provided by the professional team from *Svenska Kyrkan* and some tips given in previous researches. The data of relative humidity along the year 2015 is represented in Graph 1, where a period without measurements can clearly be seen in the middle of the graph. However, this period of missing data corresponds to summer months when the temperatures of the glasses are higher and there is lower or no risk to condensation. The gathered data consist of relative humidity measurements in the indoor air, outside the cathedral and at two different heights in the gap between panes. These two last measurements correspond to the positions 1f and 6f show in Appendix II.

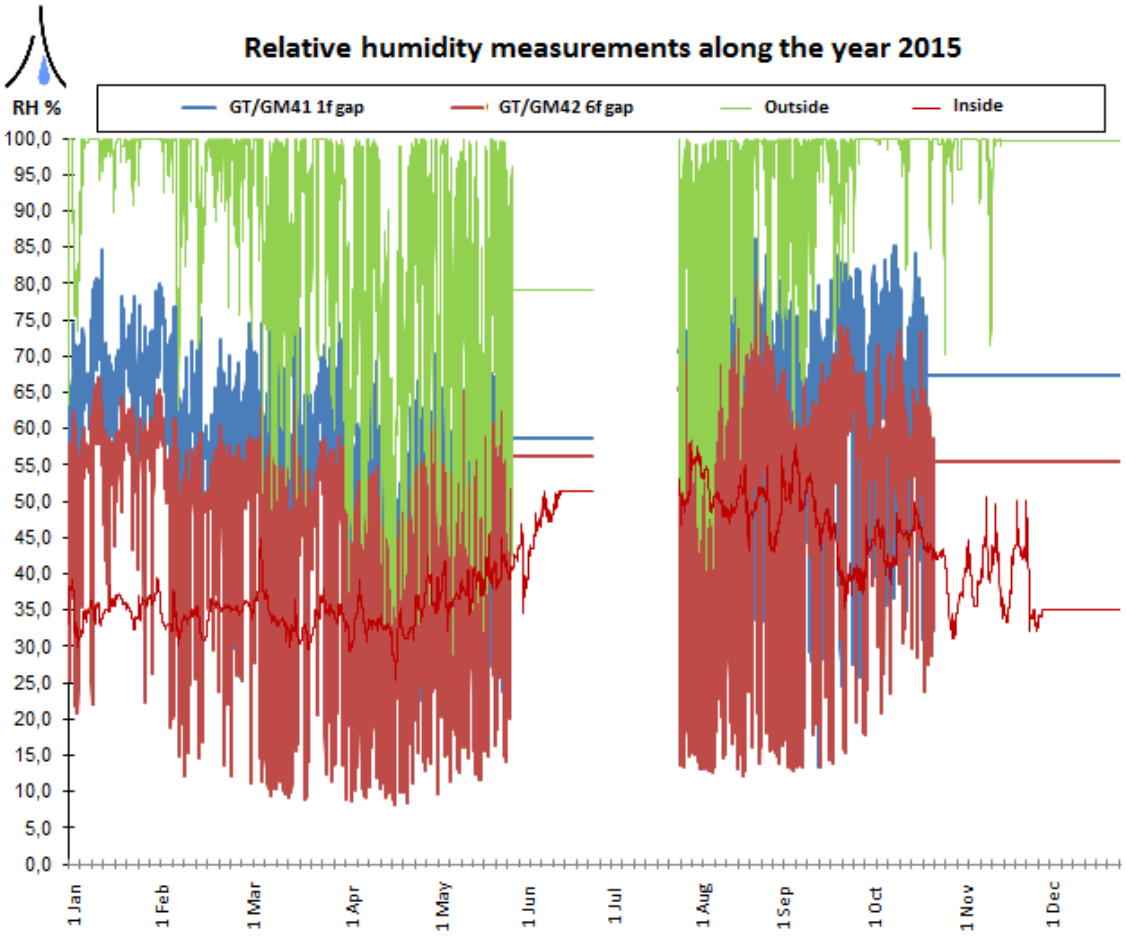

Graph 1: relative humidity measurements during the year 2015

In this analysis, the most important tip consists of the experience of a German study [19] where condensation appeared when the relative humidity in the gap exceeded the 68%. Also, regarding the clues in [15] [19] about the air velocity, the measured speeds in the air gap should also be contrasted with the recommendations provided.

An analytical study can be made from the available data; obtaining the vapour pressure out of the relative humidity (see equation (25)) and comparing the corresponding saturation temperature to the ones of the surfaces facing the gap. Every time the surfaces are at lower temperature than the saturation one, condensation appears. Besides, since there is data available at two different heights, it is possible to obtain positive results for condensation just in one part of the window

$$RH = 100 \cdot \frac{P_v}{P_{v,s}} \qquad (25)$$

Where
P_v= pressure of the vapour present in the air
$P_{v,s}$= condensation pressure at the temperature of the vapour
**Notice that both pressures need to have the same units.*

However, as it will be exhibited in the results, the limitation of a relative humidity higher than 68% is more restrictive. The reason for this is that it comes from an experimental study, which means that even though the effects of air pollutants are not strictly analysed they are inherent to the results. Provided that the limitation in the relative humidity is more restrictive along with the fact that the climate of the region where the German study was developed is similar to the one in Uppsala regarding pressure and temperature, it is rational to stablish it as the basis of the analysis.

Therefore, the time along the year when the measurements of relative humidity in the space between panes are higher than this stablished limit will be considered as the time when condensation occurs.

4. RESULTS

4.1 Results of the analysis of the improvement in thermal behavior

Since the glass temperature measurements were provided at two different locations, first the results obtained for the higher one (6f) will be exposed in detail and afterwards the overall U-factor obtained for the position 1f and the mean values of the results obtained in both cases will also be exposed.

Furthermore, the results obtained in the location 6f will be presented for different selected periods, which are the same in the three methodologies, in order to discuss as well the influence of the outside temperature in the overall U-factor.

4.1.1 Results obtained in Method 1 in location 6f

Here, the results obtained in the method consisting in the comparison of the global overall U-factors before and after the implementation of the protective glazing, which is described in section 3.2.2, are presented.

The combined heat transfer coefficient h_i for the inner surface of the stained glass and the overall U-factor for the stained glass alone, obtained with an assessed value of 30 W/m^2·K for the α_e and the conductance and the thickness of the historical glass given by the professional team from *Svenska Kyrkan* (0.8 W/m·K and 2.5 mm respectively), are presented in Table 1 for the 1st of January between 1:30 and 9:00 a.m. The results of the overall U-value of the installed obtained in this period and the ratio between the two U-factors are also presented.

Table 1: results for the heat transfer coefficients obtained using the first method and in the first period of analysis, in location 6f

	$T_{out}[°C]$	$T_{\infty}[°C]$	$h_i\left[\frac{W}{m^2K}\right]$	$U_{sg}\left[\frac{W}{m^2K}\right]$	$U_{ps}\left[\frac{W}{m^2K}\right]$	$\frac{U_{sg}}{U_{ps}}[-]$
1:30	2.51	15.70	8.00	6.19	1.57	3.95
2:00	2.85	15.70	7.98	6.18	1.56	3.96
2:30	3.01	15.70	7.97	6.18	1.56	3.96
3:00	2.95	15.70	7.98	6.18	1.56	3.95
3:30	2.73	15.70	7.99	6.18	1.58	3.93
4:00	2.37	15.70	8.00	6.20	1.59	3.91
4:30	2.01	15.49	8.00	6.19	1.59	3.89
5:00	1.76	15.49	8.01	6.20	1.59	3.89
5:30	1.73	15.49	8.01	6.20	1.59	3.89
6:00	1.73	15.49	8.01	6.20	1.60	3.88
6:30	1.76	15.49	8.01	6.20	1.60	3.88
7:00	1.87	15.49	8.00	6.20	1.59	3.89
7:30	2.04	15.49	8.00	6.19	1.60	3.87
8:00	2.21	15.49	7.99	6.19	1.59	3.90
8:30	2.44	15.49	7.98	6.18	1.57	3.93

9:00	2.68	15.49	7.97	6.17	1.56	3.95

In the following Table 2, the results obtained for the overall U-value of the system in the next selected period that goes from 13:00 to 16:30 p.m. the same day are exposed.

Table 2: results for the heat transfer coefficients obtained using the first method and in the second period of analysis, in location 6f

	$T_{out}[\,°C]$	$T_{\infty}[°C]$	$h_i\left[\frac{W}{m^2K}\right]$	$U_{sg}\left[\frac{W}{m^2K}\right]$	$U_{ps}\left[\frac{W}{m^2K}\right]$	$\frac{U_{sg}}{U_{ps}}\,[-]$
13:00	4.36	15.68	7.90	6.13	1.51	4.07
13:30	4.70	15.68	7.88	6.12	1.50	4.09
14:00	4.99	15.68	7.86	6.11	1.49	4.11
14:30	4.97	15.68	7.86	6.11	1.49	4.11
15:00	5.00	15.68	7.86	6.11	1.49	4.11
15.30	5.13	15.68	7.85	6.11	1.48	4.13
16:00	5.23	15.68	7.85	6.10	1.47	4.14
16:30	5.34	15.68	7.84	6.10	1.47	4.15

In order to study the case of negative outside temperatures, which is interesting because greater heat loss is expected and it is a common situation during winter, the period from the 1st of February at 18:30 p.m. to the 2nd of February at 00:30 a.m. has been chosen. The results can be observed in Table 3:

Table 3: results for the heat transfer coefficients obtained using the first method and in the third period of analysis, in location 6f

	$T_{out}[\,°C]$	$T_{\infty}[°C]$	$h_i\left[\frac{W}{m^2K}\right]$	$U_{sg}\left[\frac{W}{m^2K}\right]$	$U_{ps}\left[\frac{W}{m^2K}\right]$	$\frac{U_{sg}}{U_{ps}}\,[-]$
18:30	-1.48	15.41	8.13	6.27	1.65	3.81
19:00	-1.67	15.41	8.13	6.27	1.65	3.81
19:30	-1.87	15.21	8.12	6.27	1.65	3.81
20:00	-2.18	15.21	8.13	6.27	1.65	3.80
20:30	-2.33	15.21	8.14	6.28	1.65	3.80
21:00	-2.48	15.21	8.14	6.28	1.66	3.79
21:30	-2.59	15.21	8.14	6.28	1.66	3.78
22:00	-2.80	15.21	8.15	6.28	1.67	3.77
22:30	-2.94	15.21	8.16	6.29	1.67	3.77
23:00	-3.11	15.21	8.16	6.29	1.67	3.76
23:30	-3.25	15.21	8.16	6.29	1.68	3.75
00:00	-3.33	15.21	8.17	6.29	1.68	3.75
00:30	-3.31	15.13	8.16	6.29	1.67	3.76

4.1.2 Results obtained in Method 2 in location 6f

In the tables below, the results obtained in the method based on the heat balance in the control volume containing the protective glazing and the historical glass, which is described in section 3.2.3, are displayed.

For the same first period as in 4.1.1 the results obtained applying this second method are presented in Table 4 and Table 5; in the first one relevant information about the heat transfer coefficients and in the second one the quantification of the different heat transfers that take part in the balance.

Table 4: results for the heat transfer coefficients obtained using the second method and in the first period of analysis, in location 6f

	$T_{out}[\,°C]$	$T_{\infty}[\,°C]$	$h_{i.sg}\left[\frac{W}{m^2K}\right]$	$U_{ps}\left[\frac{W}{m^2K}\right]$	$\frac{U_{sg}}{U_{ps}}[-]$
1:30	2.51	15.70	7.23	1.64	3.78
2:00	2.85	15.70	7.23	1.65	3.75
2:30	3.01	15.70	7.23	1.67	3.69
3:00	2.95	15.70	7.23	1.69	3.66
3:30	2.73	15.70	7.23	1.68	3.67
4:00	2.37	15.70	7.23	1.68	3.68
4:30	2.01	15.49	7.23	1.66	3.72
5:00	1.76	15.49	7.22	1.66	3.74
5:30	1.73	15.49	7.22	1.62	3.84
6:00	1.73	15.49	7.22	1.62	3.82
6:30	1.76	15.49	7.22	1.65	3.75
7:00	1.87	15.49	7.22	1.65	3.75
7:30	2.04	15.49	7.22	1.67	3.72
8:00	2.21	15.49	7.22	1.69	3.67
8:30	2.44	15.49	7.22	1.67	3.71
9:00	2.68	15.49	7.22	1.68	3.69

Table 5: results of the heat balance obtained using the second method and in the first period of analysis, in location 6f

	$\dot{Q}_{conv+rad.sg}\left[\frac{W}{m^2}\right]$	$u_{ave}\left[\frac{m}{s}\right]$	$\dot{m}_{air}\left[\frac{kg}{s}\right]$	$\Delta\dot{Q}_{air}\left[\frac{W}{m^2}\right]$	$\dot{Q}_{e}\left[\frac{W}{m^2}\right]$
1:30	19.59	0.07	0.00261	2.48	22.07
2:00	19.59	0.07	0.00254	2.18	21.77
2:30	19.59	0.07	0.00249	1.92	21.51
3:00	19.59	0.06	0.00234	1.80	21.39
3:30	19.59	0.06	0.00241	1.86	21.45
4:00	19.59	0.07	0.00251	2.17	21.76
4:30	19.59	0.07	0.00271	2.58	22.17
5:00	19.58	0.08	0.00291	2.77	22.35
5:30	19.58	0.07	0.00274	2.60	22.18

6:00	19.58	0.08	0.00291	2.77	22.35
6:30	19.58	0.08	0.00293	3.19	22.76
7:00	19.58	0.08	0.00286	3.10	22.68
7:30	19.58	0.08	0.00289	3.13	22.71
8:00	19.58	0.08	0.00289	3.13	22.71
8:30	19.58	0.07	0.00271	2.57	22.15
9:00	19.58	0.07	0.00266	2.29	21.87

The same results are exposed in Table 6 and Table 7 for the second studied period (the same day between 13:00 and 16:30 p.m.), where the outdoor temperature is a bit higher.

Table 6: results for the heat transfer coefficients obtained using the second method and in the second period of analysis, in location 6f

	$T_{out}[\,°C]$	$T_{\infty}[\,°C]$	$h_{i.sg}\left[\frac{W}{m^2K}\right]$	$U_{ps}\left[\frac{W}{m^2K}\right]$	$\frac{U_{sg}}{U_{ps}}\,[-]$
13:00	4.36	15.68	7.16	1.52	4.06
13:30	4.70	15.68	7.10	1.43	4.29
14:00	4.99	15.68	7.10	1.48	4.15
14:30	4.97	15.68	7.10	1.49	4.09
15:00	5.00	15.68	7.10	1.49	4.10
15.30	5.13	15.68	7.05	1.36	4.49
16:00	5.23	15.68	7.05	1.38	4.41
16:30	5.34	15.68	7.05	1.38	4.41

Table 7: results of the heat balance obtained using the second method and in the second period of analysis, in location 6f

	$\dot{Q}_{conv+rad.sg}\left[\frac{W}{m^2}\right]$	$u_{ave}\left[\frac{m}{s}\right]$	$\dot{m}_{air}\left[\frac{kg}{s}\right]$	$\Delta\dot{Q}_{air}\left[\frac{W}{m^2}\right]$	$\dot{Q}_{e}\left[\frac{W}{m^2}\right]$
13:00	16.52	0.06	0.00211	1.447	17.97
13:30	14.74	0.06	0.00206	1.41	16.16
14:00	14.74	0.06	0.00211	1.45	16.19
14:30	14.74	0.05	0.00204	1.21	15.95
15:00	14.74	0.06	0.00209	1.24	15.98
15.30	13.21	0.06	0.00221	1.31	14.53
16:00	13.21	0.05	0.00204	1.39	14.60
16:30	13.21	0.06	0.00206	1.23	14.44

The results obtained for colder outside temperatures, in the period from the 1st of February at 18:30 p.m. to the 2nd of February at 00:30 a.m. can be seen in Table 8 and Table 9:

Table 8: results for the heat transfer coefficients obtained using the second method and in the third period of analysis, in location 6f

	$T_{out}[\,°C]$	$T_{\infty}[\,°C]$	$h_{i.sg}\left[\frac{W}{m^2K}\right]$	$U_{ps}\left[\frac{W}{m^2K}\right]$	$\frac{U_{sg}}{U_{ps}}\,[-]$
18:30	-1.48	15.41	7.29	1.67	3.74
19:00	-1.67	15.41	7.29	1.74	3.61
19:30	-1.87	15.21	7.28	1.73	3.63
20:00	-2.18	15.21	7.28	1.74	3.61
20:30	-2.33	15.21	7.28	1.71	3.66
21:00	-2.48	15.21	7.32	1.79	3.50
21:30	-2.59	15.21	7.32	1.78	3.52
22:00	-2.80	15.21	7.32	1.79	3.51
22:30	-2.94	15.21	7.32	1.80	3.49
23:00	-3.11	15.21	7.32	1.80	3.49
23:30	-3.25	15.21	7.35	1.90	3.31
00:00	-3.33	15.21	7.35	1.89	3.33
00:30	-3.31	15.13	7.34	1.87	3.37

Table 9: results of the heat balance obtained using the second method and in the third period of analysis, in location 6f

	$\dot{Q}_{conv+rad.sg}\left[\frac{W}{m^2}\right]$	$u_{ave}\left[\frac{m}{s}\right]$	$\dot{m}_{air}\left[\frac{kg}{s}\right]$	$\Delta\dot{Q}_{air}\left[\frac{W}{m^2}\right]$	$\dot{Q}_{e}\left[\frac{W}{m^2}\right]$
18:30	23.14	0.16	0.005819	5.13	28.26
19:00	23.14	0.16	0.005943	6.58	29.71
19:30	23.06	0.16	0.005794	6.41	29.48
20:00	23.06	0.16	0.005943	7.11	30.17
20:30	23.06	0.16	0.005869	7.00	30.06
21:00	24.69	0.16	0.005894	7.03	31.72
21:30	24.69	0.16	0.005869	7.00	31.69
22:00	24.69	0.16	0.005894	7.55	32.25
22:30	24.69	0.16	0.005844	8.01	32.71
23:00	24.69	0.16	0.006043	8.29	32.98
23:30	26.29	0.16	0.006043	8.83	35.11
00:00	26.29	0.16	0.006018	8.79	35.08
00:30	26.13	0.16	0.006068	8.26	34.39

4.1.3 Results obtained in Method 3 in location 6f

In this section, the results achieved in the third method that is based on the heat balance in the protective glass as explained in section 3.2.4 are exposed.

The results procured by this last method for the 1st of January between 1:30 and 9:00 a.m. are presented, as in the previous section, in Table 10 and Table 11, the ones obtained for the same day from 13:00 to 16:30 p.m. in Table 12 and Table 13, and the ones attained for the period from the 1st of February at 18:30 p.m. to the 2nd of February at 00:30 a.m. in Table 14 and Table 15.

Table 10: results for the heat transfer coefficients obtained using the third method and in the first period of analysis, in location 6f

	$T_{out}[\,^{\circ}\mathrm{C}]$	$T_{\infty}[\,^{\circ}\mathrm{C}]$	$h_{conv.i}\left[\frac{\mathrm{W}}{\mathrm{m^2K}}\right]$	$\mathrm{U_{ps}}\left[\frac{\mathrm{W}}{\mathrm{m^2K}}\right]$	$\frac{\mathrm{U_{sg}}}{\mathrm{U_{ps}}}\,[-]$
1:30	2.51	15.70	1.70	1.90	3.27
2:00	2.85	15.70	1.69	1.84	3.37
2:30	3.01	15.70	1.68	1.79	3.47
3:00	2.95	15.70	1.68	1.81	3.42
3:30	2.73	15.70	1.68	1.90	3.25
4:00	2.37	15.70	1.69	1.98	3.12
4:30	2.01	15.49	1.71	2.04	3.03
5:00	1.76	15.49	1.72	2.07	2.99
5:30	1.73	15.49	1.72	2.03	3.05
6:00	1.73	15.49	1.72	2.03	3.06
6:30	1.76	15.49	1.72	2.17	2.86
7:00	1.87	15.49	1.72	2.17	2.86
7:30	2.04	15.49	1.72	2.03	3.06
8:00	2.21	15.49	1.72	2.14	2.89
8:30	2.44	15.49	1.71	2.04	3.03
9:00	2.68	15.49	1.69	1.87	3.30

Table 11: results of the heat balance obtained using the third method and in the first period of analysis, in location 6f

	$\dot{Q}_{conv.i}\left[\frac{\mathrm{W}}{\mathrm{m^2}}\right]$	$\dot{Q}_{rad.ps}\left[\frac{\mathrm{W}}{\mathrm{m^2}}\right]$	$\dot{Q}_{e}\left[\frac{\mathrm{W}}{\mathrm{m^2}}\right]$
1:30	15.70	9.94	25.64
2:00	15.24	8.99	24.22
2:30	14.80	8.13	22.93
3:00	14.80	8.13	22.93
3:30	15.15	9.09	24.25
4:00	15.65	10.00	25.65
4:30	16.18	10.99	27.16
5:00	16.46	11.45	27.91
5:30	16.46	11.45	27.91
6:00	16.46	11.45	27.91
6:30	17.01	12.79	29.81
7:00	17.01	12.79	29.81

7:30	16.63	10.96	27.58
8:00	16.98	11.82	28.81
8:30	16.16	10.97	27.13
9:00	15.30	9.16	24.46

Table 12: results for the heat transfer coefficients obtained using the third method and in the second period of analysis, in location 6f

	$T_{out}[\,°C]$	$T_{\infty}[\,°C]$	$h_{conv.i}\left[\frac{W}{m^2K}\right]$	$U_{ps}\left[\frac{W}{m^2K}\right]$	$\frac{U_{sg}}{U_{ps}}\,[-]$
13:00	4.36	15.68	1.64	1.75	3.53
13:30	4.70	15.68	1.61	1.66	3.71
14:00	4.99	15.68	1.60	1.59	3.85
14:30	4.97	15.68	1.59	1.60	3.83
15:00	5.00	15.68	1.59	1.60	3.83
15.30	5.13	15.68	1.59	1.60	3.82
16:00	5.23	15.68	1.58	1.50	4.08
16:30	5.34	15.68	1.58	1.40	4.37

Table 13: results of the heat balance obtained using the third method and in the second period of analysis, in location 6f

	$\dot{Q}_{conv.i}\left[\frac{W}{m^2}\right]$	$\dot{Q}_{rad.ps}\left[\frac{W}{m^2}\right]$	$\dot{Q}_{e}\left[\frac{W}{m^2}\right]$
13:00	13.36	7.36	20.72
13:30	12.44	6.36	18.80
14:00	12.03	5.46	17.49
14:30	11.62	5.46	17.08
15:00	11.62	5.46	17.08
15.30	11.62	5.46	17.08
16:00	11.22	4.59	15.81
16:30	10.90	3.69	14.58

Table 14: results for the heat transfer coefficients obtained using the third method and in the third period of analysis, in location 6f

	$T_{out}[\,°C]$	$T_{\infty}[\,°C]$	$h_{conv.i}\left[\frac{W}{m^2K}\right]$	$U_{ps}\left[\frac{W}{m^2K}\right]$	$\frac{U_{sg}}{U_{ps}}\,[-]$
18:30	-1.48	15.41	1.80	2.34	2.68
19:00	-1.67	15.41	1.79	2.29	2.74
19:30	-1.87	15.21	1.79	2.31	2.71
20:00	-2.18	15.21	1.80	2.29	2.73
20:30	-2.33	15.21	1.81	2.28	2.75
21:00	-2.48	15.21	1.81	2.34	2.69
21:30	-2.59	15.21	1.82	2.33	2.70

22:00	-2.80	15.21	1.82	2.25	2.79
22:30	-2.94	15.21	1.81	2.23	2.82
23:00	-3.11	15.21	1.82	2.35	2.68
23:30	-3.25	15.21	1.82	2.32	2.72
00:00	-3.33	15.21	1.82	2.31	2.73
00:30	-3.31	15.13	1.82	2.31	2.72

Table 15: results of the heat balance obtained using the third method and in the third period of analysis, in location 6f

	$\dot{Q}_{conv.i}\left[\frac{W}{m^2}\right]$	$\dot{Q}_{rad.ps}\left[\frac{W}{m^2}\right]$	$\dot{Q}_{e}\left[\frac{W}{m^2}\right]$
18:30	20.99	18.49	39.48
19:00	21.07	18.05	39.12
19:30	20.91	18.53	39.44
20:00	21.39	18.49	39.88
20:30	21.51	18.49	40.00
21:00	21.99	19.35	41.34
21:30	22.06	19.36	41.41
22:00	22.01	18.49	40.5
22:30	21.96	18.49	40.45
23:00	22.82	20.15	42.97
23:30	23.03	19.73	42.76
00:00	23.06	19.73	42.79
00:30	22.81	19.78	42.59

4.1.4 Summary of results

The results of the overall U-factor obtained for location 6f in the three different methodologies are collected in Table 16, Table 17 and Table 18 for each period presented before. Besides, the results obtained for position 1f and the mean values obtained from both cases are exposed in Table 19 and Table 20.

Table 16: summary of the results obtained for the U-values in the three different methods for the first period, in location 6f

			Method 1		**Method 2**		**Method 3**	
	$T_{out}[\,°C]$	$T_{\infty}[°C]$	$U_{ps}\left[\frac{W}{m^2K}\right]$	$\frac{U_{sg}}{U_{ps}}\,[-]$	$U_{ps}\left[\frac{W}{m^2K}\right]$	$\frac{U_{sg}}{U_{ps}}\,[-]$	$U_{ps}\left[\frac{W}{m^2K}\right]$	$\frac{U_{sg}}{U_{ps}}\,[-]$
1:30	2.51	15.70	1.57	3.95	1.64	3.78	1.90	3.27
2:00	2.85	15.70	1.56	3.96	1.65	3.75	1.84	3.37
2:30	3.01	15.70	1.56	3.96	1.67	3.69	1.79	3.47
3:00	2.95	15.70	1.56	3.95	1.69	3.66	1.81	3.42
3:30	2.73	15.70	1.58	3.93	1.68	3.67	1.90	3.25
4:00	2.37	15.70	1.59	3.91	1.68	3.68	1.98	3.12

4:30	2.01	15.49	1.59	3.89	1.66	3.72	2.04	3.03
5:00	1.76	15.49	1.59	3.89	1.66	3.74	2.07	2.99
5:30	1.73	15.49	1.59	3.89	1.62	3.84	2.03	3.05
6:00	1.73	15.49	1.60	3.88	1.62	3.82	2.03	3.06
6:30	1.76	15.49	1.60	3.88	1.65	3.75	2.17	2.86
7:00	1.87	15.49	1.59	3.89	1.65	3.75	2.17	2.86
7:30	2.04	15.49	1.60	3.87	1.67	3.72	2.03	3.06
8:00	2.21	15.49	1.59	3.90	1.69	3.67	2.14	2.89
8:30	2.44	15.49	1.57	3.93	1.67	3.71	2.04	3.03
9:00	2.68	15.49	1.56	3.95	1.68	3.69	1.87	3.30

Table 17: summary of the results obtained for the U-values in the three different methods for the second period, in location 6f

			Method 1		Method 2		Method 3	
	$T_{out}[\,°C]$	$T_{\infty}[°C]$	$U_{ps}\left[\frac{W}{m^2K}\right]$	$\frac{U_{sg}}{U_{ps}}\,[-]$	$U_{ps}\left[\frac{W}{m^2K}\right]$	$\frac{U_{sg}}{U_{ps}}\,[-]$	$U_{ps}\left[\frac{W}{m^2K}\right]$	$\frac{U_{sg}}{U_{ps}}\,[-]$
13:00	4.36	15.68	1.51	4.07	1.52	4.06	1.75	3.53
13:30	4.70	15.68	1.50	4.09	1.43	4.29	1.66	3.71
14:00	4.99	15.68	1.49	4.11	1.48	4.15	1.59	3.85
14:30	4.97	15.68	1.49	4.11	1.49	4.09	1.60	3.83
15:00	5.00	15.68	1.49	4.11	1.49	4.10	1.60	3.83
15.30	5.13	15.68	1.48	4.13	1.36	4.49	1.60	3.82
16:00	5.23	15.68	1.47	4.14	1.38	4.41	1.50	4.08
16:30	5.34	15.68	1.47	4.15	1.38	4.41	1.40	4.37

Table 18: summary of the results obtained for the U-values in the three different methods for the third period, in location 6f

			Method 1		Method 2		Method 3	
	$T_{out}[\,°C]$	$T_{\infty}[°C]$	$U_{ps}\left[\frac{W}{m^2K}\right]$	$\frac{U_{sg}}{U_{ps}}\,[-]$	$U_{ps}\left[\frac{W}{m^2K}\right]$	$\frac{U_{sg}}{U_{ps}}\,[-]$	$U_{ps}\left[\frac{W}{m^2K}\right]$	$\frac{U_{sg}}{U_{ps}}\,[-]$
18:30	-1.48	15.41	1.65	3.81	1.67	3.74	2.34	2.68
19:00	-1.67	15.41	1.65	3.81	1.74	3.61	2.29	2.74
19:30	-1.87	15.21	1.65	3.81	1.73	3.63	2.31	2.71
20:00	-2.18	15.21	1.65	3.80	1.74	3.61	2.29	2.73
20:30	-2.33	15.21	1.65	3.80	1.71	3.66	2.28	2.75
21:00	-2.48	15.21	1.66	3.79	1.79	3.50	2.34	2.69
21:30	-2.59	15.21	1.66	3.78	1.78	3.52	2.33	2.70
22:00	-2.80	15.21	1.67	3.77	1.79	3.51	2.25	2.79
22:30	-2.94	15.21	1.67	3.77	1.80	3.49	2.23	2.82
23:00	-3.11	15.21	1.67	3.76	1.80	3.49	2.35	2.68
23:30	-3.25	15.21	1.68	3.75	1.90	3.31	2.32	2.72

00:00	-3.33	15.21	1.68	3.75	1.89	3.33	2.31	2.73
00:30	-3.31	15.13	1.67	3.76	1.87	3.37	2.31	2.72

Given the fact that the results obtained in 1f are different from the ones obtained in 6f (see these locations of the sensors in Appendix II) in the two last methods of analysis, the results for the location 1f and the mean value of the results obtained in both locations are shown in the following tables Table 19 and Table 20, just for the first period of analysis.

Table 19: summary of the results obtained for the U-values in the two last different methods for the first period, in location 1f

			Method 2		Method 3	
	$T_{out}[\,°C]$	$T_{\infty}[°C]$	$U_{ps}\left[\frac{W}{m^2K}\right]$	$\frac{U_{sg}}{U_{ps}}\,[-]$	$U_{ps}\left[\frac{W}{m^2K}\right]$	$\frac{U_{sg}}{U_{ps}}\,[-]$
1:30	2.51	15.70	2,77	2,24	1,71	3,64
2:00	2.85	15.70	2,81	2,20	1,71	3,62
2:30	3.01	15.70	2,74	2,25	1,64	3,77
3:00	2.95	15.70	2,77	2,23	1,66	3,71
3:30	2.73	15.70	2,77	2,23	1,61	3,83
4:00	2.37	15.70	2,75	2,25	1,75	3,52
4:30	2.01	15.49	2,69	2,30	1,86	3,33
5:00	1.76	15.49	2,67	2,32	1,93	3,20
5:30	1.73	15.49	2,62	2,36	1,90	3,26
6:00	1.73	15.49	2,62	2,37	1,90	3,27
6:30	1.76	15.49	2,76	2,25	1,90	3,27
7:00	1.87	15.49	2,77	2,24	1,84	3,38
7:30	2.04	15.49	2,79	2,22	1,85	3,35
8:00	2.21	15.49	2,82	2,20	1,88	3,30
8:30	2.44	15.49	2,81	2,20	1,81	3,43
9:00	2.68	15.49	2,71	2,28	1,75	3,53

Table 20: mean values of the results obtained for the overall U-factors in both locations using the two last methods for the first period

			Method 2		Method 3	
	$T_{out}[\,°C]$	$T_{\infty}[°C]$	$U_{ps}\left[\frac{W}{m^2K}\right]$	$\frac{U_{sg}}{U_{ps}}\,[-]$	$U_{ps}\left[\frac{W}{m^2K}\right]$	$\frac{U_{sg}}{U_{ps}}\,[-]$
1:30	2.51	15.70	2,21	2,81	1,81	3,44
2:00	2.85	15.70	2,23	2,77	1,77	3,49
2:30	3.01	15.70	2,21	2,80	1,71	3,61
3:00	2.95	15.70	2,23	2,77	1,74	3,56
3:30	2.73	15.70	2,22	2,78	1,76	3,52
4:00	2.37	15.70	2,22	2,79	1,87	3,31
4:30	2.01	15.49	2,18	2,85	1,95	3,17

5:00	1.76	15.49	2,16	2,87	2,00	3,09
5:30	1.73	15.49	2,12	2,93	1,97	3,15
6:00	1.73	15.49	2,12	2,92	1,96	3,16
6:30	1.76	15.49	2,21	2,81	2,03	3,05
7:00	1.87	15.49	2,21	2,80	2,00	3,09
7:30	2.04	15.49	2,23	2,78	1,94	3,20
8:00	2.21	15.49	2,25	2,75	2,01	3,09
8:30	2.44	15.49	2,24	2,76	1,92	3,22
9:00	2.68	15.49	2,19	2,82	1,81	3,41

4.1.5 Results of the estimation of the energy savings

On the one hand, using the values of the overall U-factor for the installed protective system provided by the first method and the equation (24) in section 3.2.5 the estimation of the energy savings obtained can be seen in Table 21:

Table 21: estimation of the energy savings achieved with the protective glazing system using method 1

	$\dot{Q}_{saved}$ [kWh/year]
Sonens fönster	9682.75
Rosette	5463.49
Both windows	15146.24

On the other hand, using a ratio U_{sg}/U_{ps} of around 3 instead (value derived from the observation of the results provided by the two last methods which take into account the radiation emitted from the interior of the cathedral), the estimation of the energy savings is the one appearing in Table 22:

Table 22: estimation of the energy savings achieved with the protective glazing system using a ratio U_{sg}/U_{ps} of 3

	$\dot{Q}_{saved}$ [kWh/year]
Sonens fönster	8699.49
Rosette	4908.68
Both windows	13608.17

4.2 Results of the evaluation of the risk of condensation in the new system

The temperatures measured by the lower sensor (1f) implicated in the analysis, in a period containing a fraction of time when the RH exceeds the limit of 68% are represented in the Graph 2 below.

In addition, the results obtained in the analytical analysis in a short period where the relative humidity registered by the lower sensor in the gap exceeds the limit of 68% are presented in the following Table 23. The period considered, the 4th of January in

the early morning, has been selected regarding that its values of RH are some of the highest obtained analytically.

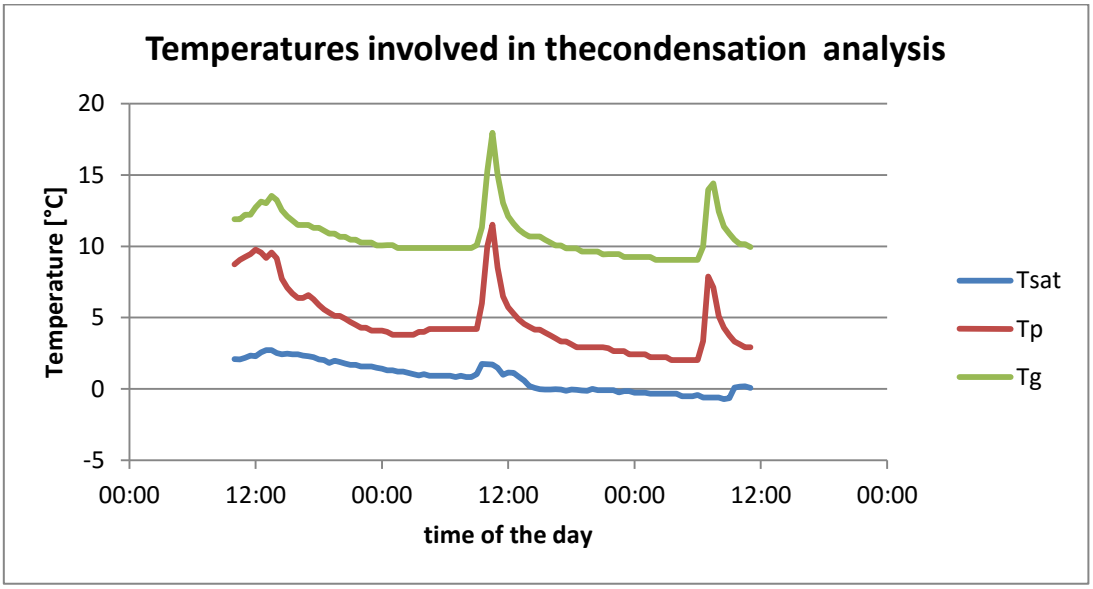

Graph 2: representation of the three temperatures involved in the condensation problem

Table 23: results of the analytical analysis of condensation in a critical period

	$RH[\,\%]$	$T_{air}[\,°C]$	$P_v[\,kPa]$	$T_{sat}[°C]$	$T_p[\,°C]$	$T_g[\,°C]$
00:30	70.19	4.67	0.598	-0.25	2.44	9.26
01:00	70.19	4.67	0.598	-0.25	2.44	9.26
01:30	70.70	4.47	0.594	-0.33	2.23	9.26
02:00	70.70	4.47	0.594	-0.33	2.23	9.06

Also, the percentage of time when the relative humidity measured by the upper (6f) and the lower (1f) sensors exceeds the limit can be seen in Table 245:

Table 24: results of the estimation of the fraction of time that the glass is exposed to condensation

	% of time
1f	29.66
6f	6.20

5. DISCUSSION

Since the heat transfer through the window depends strongly on the natural convection in the space between the panes and the air flow is driven by the buoyancy provoked by the temperature difference between the inner surface of the outer pane and the indoor air, different temperatures lead to different overall U-factors.

This certainty can be noticed in the tables of results displayed for location 6f. Regardless the methodology, with the indoor temperature varying less than 0.6°C due to the installed controlled system of heating and ventilation, lower outside temperatures lead to higher overall heat transfer coefficients of the system. As a result, the ratio U_{sg}/U_{ps} is lower, which means that less improvement in the thermal behavior is achieved and therefore less energy is saved in the heating system. However, there still are important savings given the fact that the lowest ratio obtained is still greater than 3 for location 6f and close to 3 in the case of calculations of mean values derived from the results obtained for both positions of the sensors. Consequently, provided that the summer of 2015 was considerably warm in comparison with other years, in future estimations of energy savings this relation between the outdoor temperature and the overall U-factor must be taken into account. In relation to this, it is useful to observe in the obtained results that even though the ratio U_{sg}/U_{ps} decreases when the outdoor temperature does so too, its variation is not that big.

In addition, the three different methodologies clearly provide distinct values for the overall heat transfer coefficient of the installed system. First of all, it must be taken into account that the first methodology does not consider radiation while the other two consider it even though they do it through different ways of analysis. Therefore, differences in the results obtained through this methodology and the other two are expected and legitimate. However, the two last methodologies provide different results from one another too and in fact their results differ more than the ones of the first from the ones of the second methodology, as it can be observed in Table 16, Table 17 and Table 18 displayed in the section of summary of results. This fact is the evidence of an error that has two main sources.

On the one hand, in these two last methodologies that are based in a heat balance, there are simplifications inherent to the equations used to quantify the different heat transfers and some values, such as physical properties of both glasses, are not known but assumed and accepted as accurate enough.

On the other hand, the different parameters involved in the heat transfer calculations depend strongly on the measured data e.g. the global heat transfer coefficient of radiation and convection of a surface and the mass flow of air completely depend on the temperature and the air velocity data respectively. Therefore, the functioning and configuration of the sensors have a big influence in the results, and methodologies like the first one presented which depends on fewer of this data are less perturbed by occasional failures in the data gathering such as the misreading of one or various sensors or the desynchronizing of their measurements.

The matter of discussion in this case, is which methodology between the ones considering radiation is the most reliable. Given the importance of natural convection over radiation in the phenomenon occurring in this problem, the fact that the U_{sg}/U_{ps} ratios obtained in the second methodology follow a similar tendency to that of the ones procured by the first methodology is a sign of good performance. Accordingly, the second methodology, this is; the one analysing the control volume containing both glasses, seems to be more solid than the third one. Besides, it is more stable to variations in the outdoor temperature and thus, if it really is more accurate than the third one, it means that the system has a better performance at low outside temperatures than it seems with the results obtained in the third one. Nevertheless, the only way to assess if the method really is more solid is to submit the system to an experimental test, as the one carried out in [1].

In addition, it would be good to asses if this second methodology, that uses real measured data and different heat transfer equations, is more or less valid than the first one which considers only natural convection but has been developed analytically from differential equations of fluid mechanics and is supported by experts in the matter and previous similar studies. However, it is hard to know.

On the one hand, the results obtained in the first methodology are comparable to the ones obtained in the previous study on a stained glass and protective glazing system at a Swiss parish church. Values of 5.78 W/m^2·K and 1.68 W/m^2·K [1] were published for the overall U-factor of the stained glass and the ventilated system installed with the protective glazing respectively, which gives a ratio U_{sg}/U_{ps} of 3.44. However, the conditions of the experiment may not be the most appropriate to simulate the ones of the Uppsala cathedral, and given the strong influence of natural convection and hence of the glass temperatures in the thermal behavior of the window the results published in [1] may be orientative but not conclusive. Besides, in [21] U-values more similar to the ones obtained in Table 20 are given for double paned windows. In that paper [21] values below 2 W/m^2·K are considerably low and related to windows filled with argon or with some kind of insulation.

Therefore, the fact that the U-values obtained using method 1 may be too low makes it reasonable to estimate the energy savings with a ratio U_{sg}/U_{ps} of 3 instead. Hence, the estimation is less likely to be undesirably optimistic.

Regarding the condensation problem, some observations can be made. Firstly, in Graph 2 it can be seen that for considerably high relative humidity of the air between panes the saturation temperature is still a bit lower than the temperatures of the surfaces facing the gap. Therefore, if it was not for the substances (dust and air pollutants) altering the dew point condensation would not be expected. The temperatures involved and the corresponding values of relative humidity registered in the midplane of the gap are given in Table 23 for a short period when the situation is more critic. Nevertheless, there is a source of error in the fact that the temperature and relative humidity of the air have been measured only in the midplane of the space between panes. In reality, there is a horizontal distribution of temperature and relative

humidity which leads to the need to consider different dew points for the surface of the protective glass and for the one of the stained historical glass.

Secondly, since in the installed system the glass in contact with the outdoor air is the protective glazing, and the historical glass is located in an inner position, the surface of the protective glass facing the gap is colder than the one of the stained glass. Consequently, its temperature is closer to that of saturation and therefore condensation is more likely to occur on the surface of the protective glazing than on the one of the stained glass. This, along with the fact that the temperature of the air also is lower in the region close to the protective glazing, which leads to higher RH of the air in this area, means that for the most critic periods, even analytically, condensation could have been assessed.

In addition, as the inner surface of the stained glass is at higher temperature than the one facing the gap the appearing of condensation is even less probable. As a result, in the installed system the historical glass is more protected from condensation and this will surely provide a reduction in the need of maintenance and reformation.

Finally, the results presented in Table 24 show an estimation of the percentage of the time that condensation occurred in the system during the year 2015. In order to assess the effectiveness in the reduction of condensation on the glasses, data from the case of the stained glass alone would be needed.

6. CONCLUSIONS

To start with, due to the importance of natural convection in the thermal performance of the system, its efficiency strongly depends on the outdoor and indoor temperatures. Consequently, the overall U-factor varies along the year. Nevertheless, the type and configuration of protective system studied provides a high reduction in the losses through the windows where it is installed during the whole year; according to the results obtained in the analysis (that match with the ones published in previous researches) it yields more than a three times reduction.

In addition, after applying three different methodologies of analysis, the first one based on a thorough development of differential equations of fluid dynamics and heat balances and the second one consisting in a heat balance of the whole system have given similar and more stable and reliable results for the assessment of the improvement in the thermal behavior than the third one.

As a result, although it is known that the improvement of the roof and walls is a more effective measure, and even more the reduction of the indoor temperature [10], estimations of the energy savings of 8700 kWh/year in the case of only providing the large window with the protective system and of 13000 kWh/year in the case of also installing it in the round window clearly show that the energy savings are still important. Accordingly, the implementation of the system offers a considerable energy saving in the long term, and also money savings depending on the cost of the heat delivered by the heating system of the cathedral.

Additionally, the stained glass has been proved to be in better conditions to avoid condensation in the installed system than in its original location; it is clearly less exposed to condensation on both sides and especially on the outer surface. Accordingly, the protective glazing system also reduces the need of maintenance and reformation, which was the first motivation for its implementation.

7. CONSIDERATIONS FOR FURTHER STUDIES

On the one hand, the effect of the edges and frames, which have not been considered in this study, is to increase the losses through the window. Accordingly, the real U factors are most probably higher than the ones obtained in the present analysis. In order to have more accurate information about the heat losses in both cases, further studies using temperature measurements in more locations on all the glass surfaces and considering the effect of the frames and edges could be accomplished.

On the other hand, the condensation problem has been slightly studied. A more accurate research on the condensation problem could surely be performed, and a good option would be to use the tool described in [22] since it directly measures condensation and as the experts explain in the article; the indirect method traditionally used to quantify condensation through the measurement of thermo-hygrometric parameters of the air and the surface is not as accurate as expected due to errors provided both by the instrumentation itself and environmental conditions. This, along with the analysis of the subjection of the glass to high temperatures remains for further studies of the system.

REFERENCES

[1] S. Wolf, S. Trümpler, K.G. Wakili, B. Binder, E. Baumman. “Protective Glazing: The Conflict Between Energy-Saving and Conservation Requirements”. Presented at the RECENT ADVANTAGES IN GLASS, STAINED-GLASS, AND CERAMICS CONSERVATION conference, Amsterdam, the Netherlands, 2013.

[2] G. Desrayaud, G. Lauriat. (2004). “A Numerical Study of Natural Convection in Partially Open Enclosures with a Conducting Side-Wall”. *Journal of Heat Transfer,* Vol.126, pp. 76 – 83.

[3] Sparrow, E. M., Shah, S., and Prakash, C. (1980). "Natural Convection in a Vertical Channel: I. Interacting Convection and Radiation. II. The Vertical Plate With and Without Shrouding". *Numerical Heat Transfer*, Vol. 3, pp. 297-314

[4]Sparrow, E.M., Chrysler, G.M., Azevedo, L.F. “Observed Flow Reversals and Measured-Predicted Nusselt Numbers for Natural Convection in a One-Sided Heated Vertical Channel”.*Journal of Heat Transfer,* Vol. 106, pp. 325 – 332.

[5] CVMA Project Web site, http://www.cvma.ac.uk/about/index.html

[6] L. Kvarnström, E. Andersson. “Åtgärdsförslag Skyddsglas etapp 2 Sonens fönster, s12, Uppsala Domkyrka”. *Åtgärdsförslag.* Svenska kyrkan, Jun. 2015.

[7] Y.A. Çengel, A.J. Ghajar. “Chapter 9: Natural Convection” in *Heat and Mass Transfer,* 3rd edition, Ed. New York: McGraw-Hill, 2010.

[8] Y.L. Chan, C.L. Tien. (1985) “A Numerical Study of Two-Dimensional Natural Convection in Square Open Cavities” *Heat transfer,* Vol.8, pp. 65 – 80.

[9] E. Zimmerman, A. Acharya. (1987) “Free Convection Heat Transfer in a Partially Divided Vertical Enclosure With Conducting End Wall”. *International Journal of Heat and Mass transfer,* Vol.30, nº2, pp. 319 – 331.

[10] AMERICAN SOCIETY OF HEATING, REFRIGERATING AND AIR-CONDITIONING ENGINEERS. (2009). *2009 ASHRAE handbook: fundamentals*. Atlanta, GA, American Society of Heating, Refrigeration and Air-Conditioning Engineers. http://app.knovel.com/hotlink/toc/id:kpASHRAE37/2009-ashrae-handbook

[11] H. Romich. (2004, Jan.). “EVALUATION OF PROTECTIVE GLAZING SYSTEMS”. *e-PRESERVATIONSience.* [Online] Available: http://www.morana-rtd.com/e-preservationscience/ [March. 18, 2016]. Vol.1, pp.1 – 8.

[12] K. Gysels, et. al. (2004). “Indoor Environment and Conservation in the Royal Museum of Fine Arts, Antwerp, Belgium”.*Journal of Cultural Heritage,* Vol.5, nº2, pp. 221 – 230.

[13] R.H.M. Godoi, V. Kontozova, R.V. Grieken. (2006). "The Shielding Effect of the Protective Glazing of Historical Stained Glass Windows From an Atmospheric Chemistry Perspective: Case Study Sainte Chapelle, Paris". *Atmospheric Environment,* Vol.40, pp. 1255 – 1265.

[14] M. Torge, M. Bücker, I. Feldmann. (2013). "The Effect of Climate and Particle Deposition on the Preservation of Historic Stained-glass Windows – In Situ Measurements and Laboratory Experiments". *Corpus Vitrearum.*

[15] A. Bernardi, et al., (2012, Nov.). "Conservation of stained glass windows with protective glazing: Main results from the European VIDRIO research programme". *Journal of Cultural Heritage*. [Online] Available: https://www.researchgate.net [March. 18, 2016]. Vol.14, n.6, 527 – 536.

[16] S. Oidtman, (1994). "Die Schutzverglasung – eine wirksame Schutzmabnahme gegen die Korrosion an wertvollen Glasmalerien". *Techniske Universiteit Eindhoven.*

[17] Tecnun site: http://www4.tecnun.es/

[18] P.J. Pritchard. "Chapter 8: Internal Incompressible Viscous Flow" in *Fox and McDonlads' Introduction to Fluid mechanics,* 8th edition, Ed. John Willey & Sons Inc, 2011.

[19] Oidtmann, S., Leissner, J., & Römich, H. (2000). Protective glazing. Hämtat från CVMA Great Britain: http://www.cvma.ac.uk/conserv/glazing.html

[20] https://upload.wikimedia.org/wikiversity/en/thumb/0/00/IF2_me.png/

[21]https://www.pilkington.com/~/media/Pilkington/Site%20Content/UK/Reference/TableofDefaultUValues.ashx

[22] A. Bernardi, et al. (2012) "Conservation of Stained Glass Windows: An Use-Friendly Portable Device Coming from the EU-VIDRIO Project". *Journal of Environmental Science and Engineering B,* Vol.1, pp. 519 – 526.

APPENDIX I: top view of the cathedral

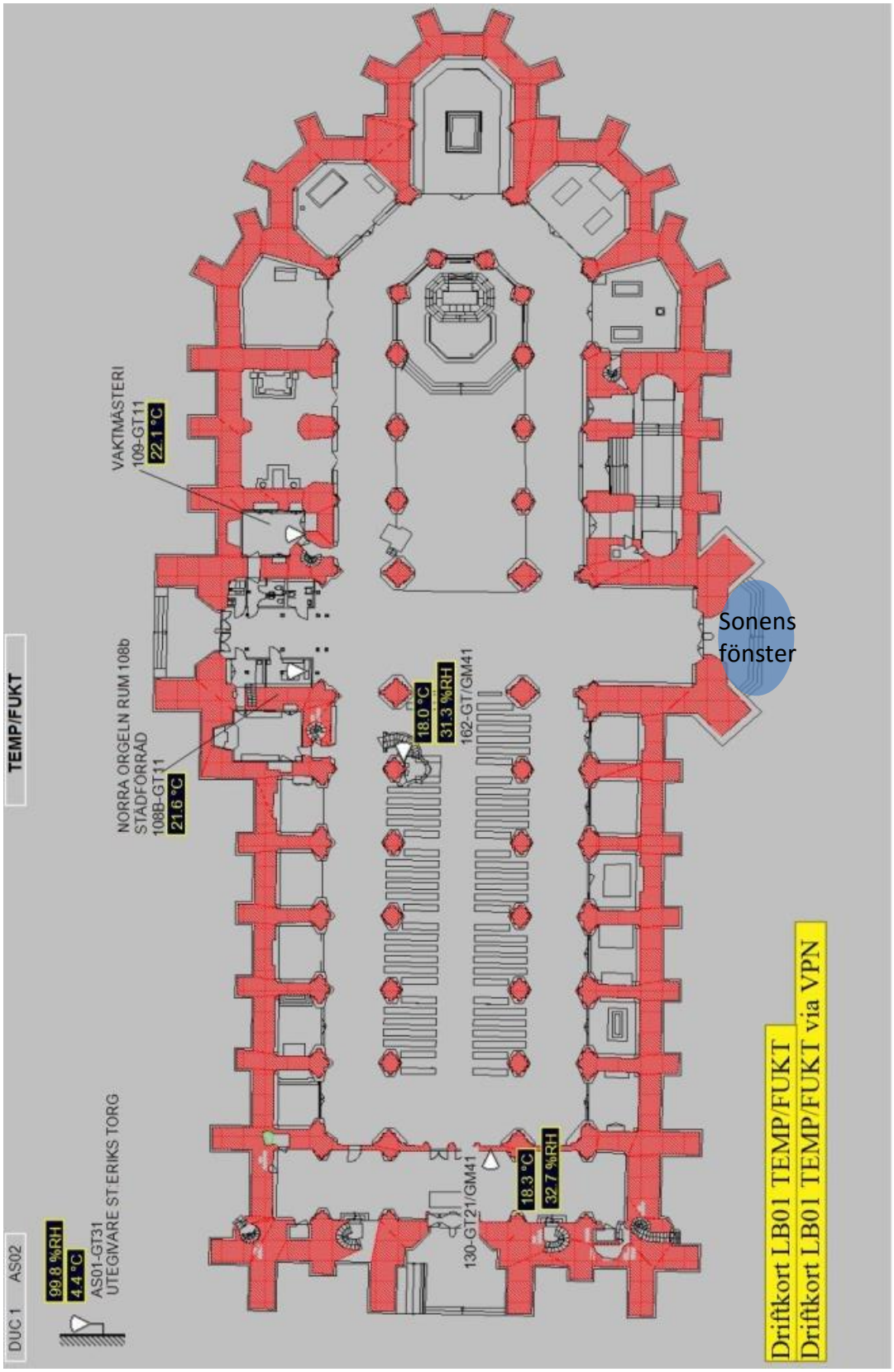

APPENDIX II: location of the different sensors

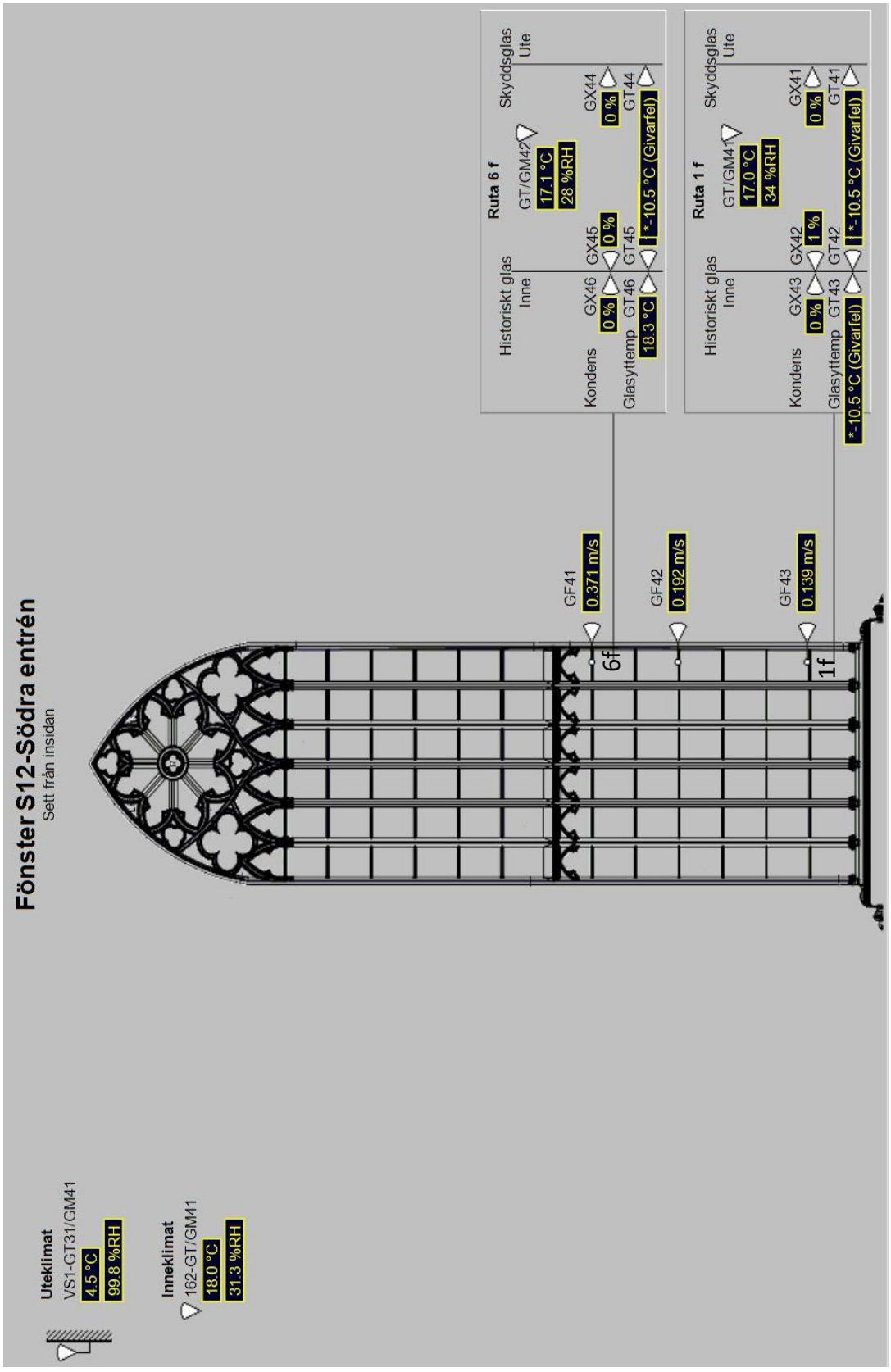

APPENDIX III: schema of the windows and estimation of dimensions

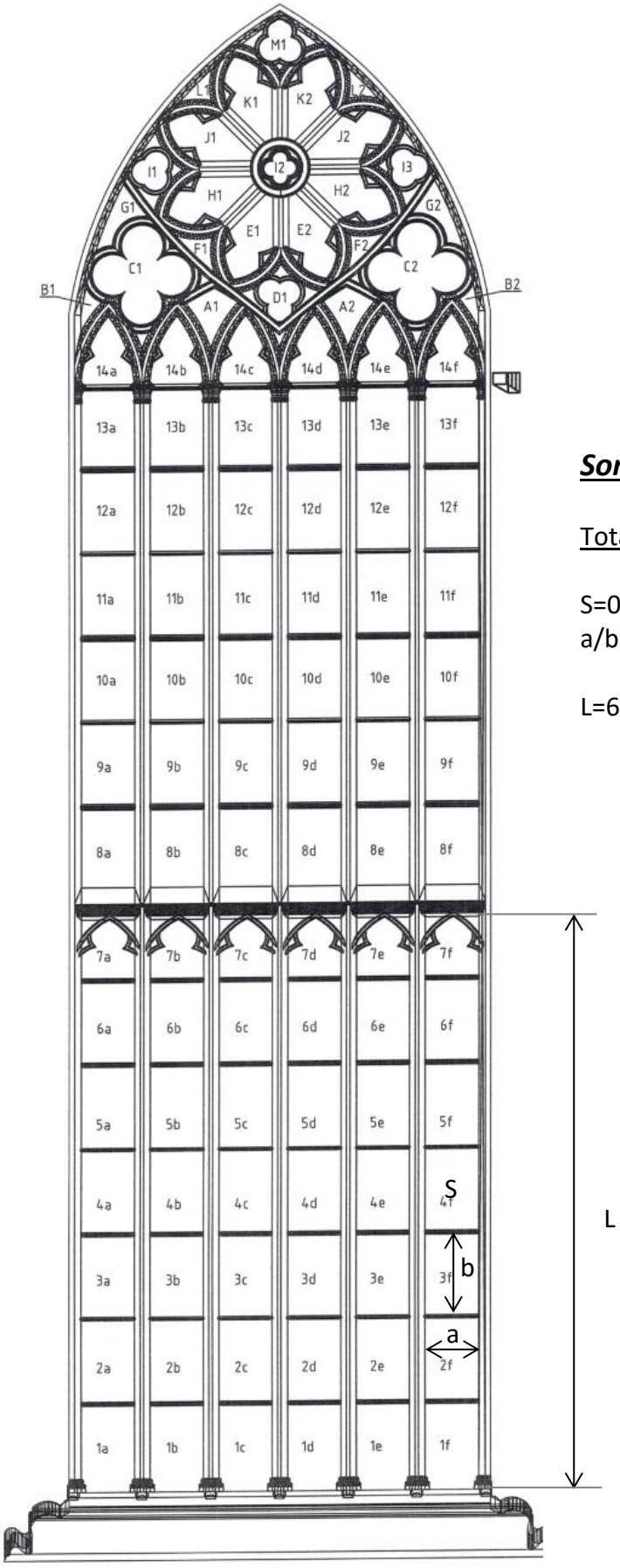

Sonens fönster

Total area: 33.1272 m^2

S=0.376198=a·b
a/b=1.1/1.7
} a=0.4934 m ; b=0.7625 m

L=6·b+1.3·b/1.7=5.158 m

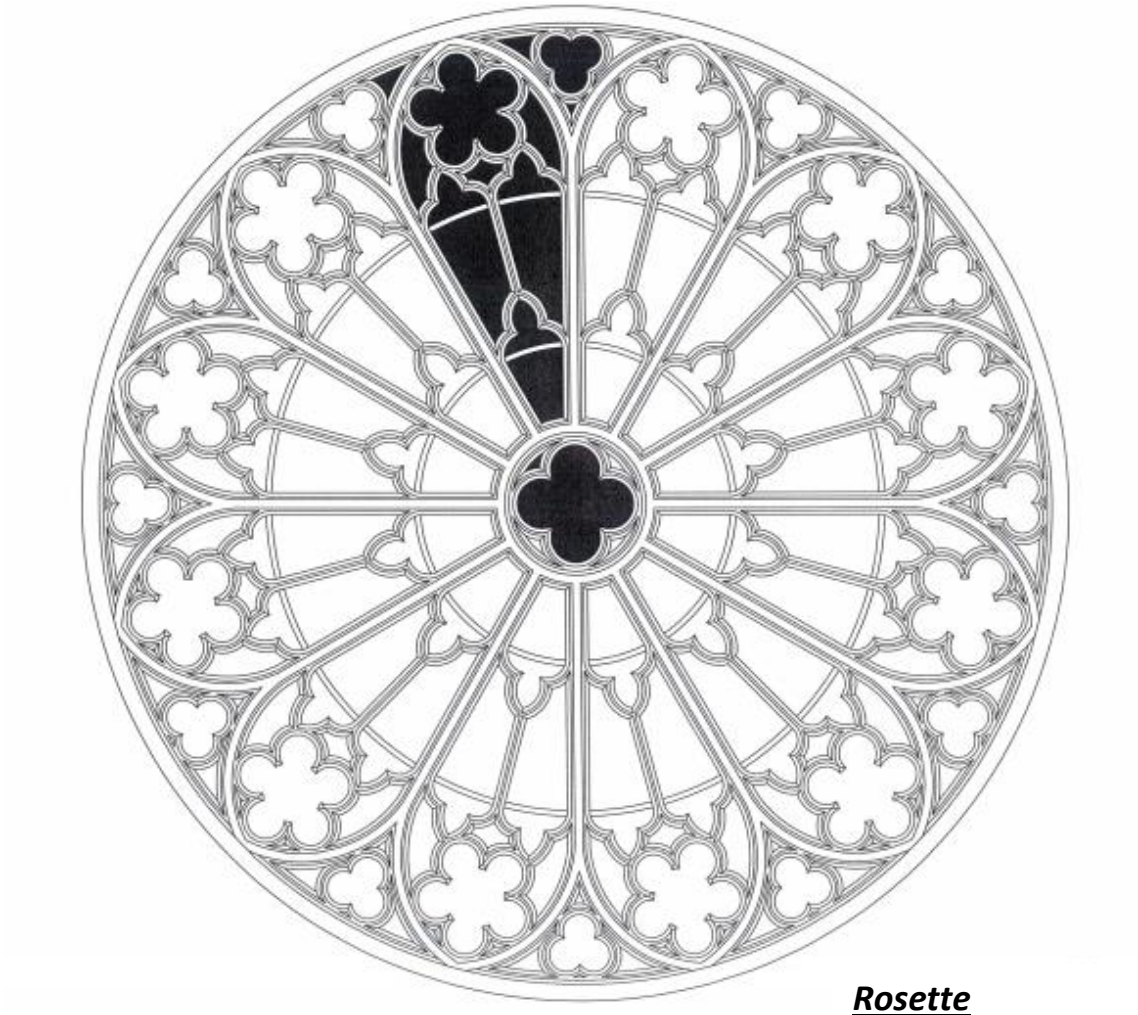

Rosette

Total area: 18.692 m^2